An assessment of ocean alkalinity enhancement using aqueous hydroxides: kinetics, efficiency, and precipitation thresholds

Mallory C. Ringham [1], Nathan Hirtle [1], Cody Shaw [1], Xi Lu [1], Julian Herndon [2,3], Brendan R. Carter [2,3], Matthew D. Eisaman [4,5]

[1] Stony Brook University, Stony Brook, NY, USA
[2] Cooperative Institute for Climate Ocean and Ecosystem Studies, University of Washington, Seattle, USA
[3] Pacific Marine Environmental Laboratory, National Oceanic and Atmospheric Administration, Seattle, WA, USA*
[4] Department of Earth & Planetary Sciences, Yale University, New Haven, CT, USA
[5] Yale Center for Natural Carbon Capture, Yale University, New Haven, CT, USA

Correspondence to: Mallory Ringham (mallory.ringham@stonybrook.edu); Current address: Ebb Carbon Inc., San Carlos, CA, USA

Abstract

Ocean alkalinity enhancement (OAE) is a promising approach to marine carbon dioxide removal (mCDR) that leverages the large surface area and carbon storage capacity of the oceans to sequester atmospheric CO_2 as dissolved bicarbonate (HCO_3^-). One OAE method involves the conversion of salt in seawater into aqueous alkalinity (NaOH), which is returned to the ocean. The resulting increase in seawater pH and alkalinity causes a shift in dissolved inorganic carbon (DIC) speciation toward carbonate and a decrease in the surface-ocean pCO_2. The shift in the pCO_2 results in enhanced uptake of atmospheric CO_2 uptake by the seawater due to gas exchange. In this study, we systematically test the efficiency of CO_2 uptake in seawater treated with NaOH at aquaria (15L) and tank (6000L) scales to establish operational boundaries for safety and efficiency in advance of scaling up to field experiments. CO_2 equilibration occurred on order of weeks to months, depending on circulation, air forcing, and air bubbling conditions within the test tanks. An increase of ~0.7-0.9 mol DIC/ mol added alkalinity (in the form of NaOH) was observed through analysis of seawater bottle samples and pH sensor data, consistent with the value expected given the values of the carbonate system equilibrium calculations for the range of salinities and temperatures tested. Mineral precipitation occurred when the bulk seawater pH exceeded 10.0 and $\Omega_{aragonite}$ exceeded 30.0. This precipitation was dominated by $Mg(OH)_2$ over hours to 1 day before shifting to $CaCO_{3,\ aragonite}$ precipitation. These data, combined with models of the dilution and advection of alkaline plumes, will allow for estimation of the amount of carbon dioxide removal expected from OAE pilot studies. Future experiments should better approximate field conditions including sediment interactions, biological activity, ocean circulation, air-sea gas exchange rates, and mixing-zone dynamics.

Keywords

Ocean Alkalinity Enhancement (OAE); marine carbon dioxide removal (mCDR); ocean carbon dioxide removal (ocean CDR)

1 Introduction

The Sixth Assessment Report of the Intergovernmental Panel on Climate Change reported that in addition to a drastic decrease in CO_2 emissions, active removal of 5-15 Gt of atmospheric CO_2 per year by 2100 is necessary to constrain average global warming to less than 1.5 - 2 °C (noting that the magnitude of carbon removals varies by

42 climate scenario: IPCC, 2022; Rogelj, 2018). A wide variety of negative emissions technologies (NETs) are under
43 development to meet this enormous challenge (Minx et al., 2018; NASEM, 2019; NASEM, 2021; Rueda et al.,
44 2021; Vitillo et al., 2022).

45 A suite of promising approaches to CO_2 removal termed ocean or marine carbon dioxide removal (ocean CDR or
46 mCDR, respectively) leverage the enormous surface area and carbon storage capacity of the ocean (Boettcher et al.,
47 2019; NASEM, 2021). Ocean alkalinity enhancement (OAE) is an mCDR method that aims to store atmospheric
48 CO_2 in a dissolved phase in the ocean as bicarbonate ions (HCO_3^-), thereby accelerating a natural planetary CO_2
49 regulation mechanism, the carbonate-silicate cycle (Berner, 1983; Isson et al., 2020). OAE has the potential to scale
50 to gigatons of CO_2 removal per year (He and Tyka, 2023), but development of this approach requires careful
51 consideration of: the methods and materials used to source and process alkalinity; the form and method of delivery
52 of alkalinity to the surface ocean (for example, aqueous or solid phase); and selection of appropriate geographic sites
53 for alkalinity dispersal (Oschlies et al., 2023). OAE methods under exploration include: mining and crushing
54 alkaline minerals (e.g., olivine, basalts) to be spread via ship or in coastal environments (e.g., beach restoration, or
55 salt marsh distribution) (Feng et al., 2017; Köhler, Hartmann, and Wolf-Gladrow, 2010; Monserrat et al., 2018;
56 Rigopoulos et al., 2018); the mining or industrial production of $Mg(OH)_2$ or mining $CaCO_3$ and calcining it to CaO
57 or $Ca(OH)_2$, with the $Mg(OH)_2$ or $Ca(OH)_2$ spread via ship or coastal outfall pipe (Harvey, 2008; Ilyina et al., 2013;
58 Kheshgi, 1995; La Plante, 2023; Moras et al., 2022; Nduagu, 2012; Rau, 2008; Renforth and Henderson, 2017;
59 Shaw, 2022); and the electrochemical conversion of saltwater into aqueous hydroxides and dispersal via coastal
60 outfalls (de Lannoy et al., 2018; Eisaman et al., 2018; Lu et al., 2022; Tyka, Van Arsdale, and Platt, 2022; Eisaman
61 et al., 2023).

62 Many of these approaches and technologies are at a nascent stage. We must move quickly to quantitatively test and
63 characterize their performance to determine which, if any, justify larger-scale deployment. The electrochemical
64 conversion of salt (NaCl) into aqueous alkalinity (NaOH) has many potential advantages in scaling considerations,
65 including simplified distribution of a liquid product to the ocean, avoidance of mining and the transportation of the
66 alkalinity source over long distances, and avoidance of potentially harmful impurities present in mined alkalinity
67 sources (NASEM, 2021; Caserini, Storni, and Grosso, 2022).

68 Total alkalinity (TA) is defined as the excess of proton acceptors over proton donors in an aqueous solution (Eq. 1),
69 where ellipses represent neglected acids and bases (Dickson 1981; Dickson 1992; Wolf-Gladrow et al., 2007). A
70 higher TA value for a seawater sample indicates that it has a higher buffering capacity than a sample with a lower
71 TA value. That is, for sample with a higher TA value, the addition of a given amount of acid to the sample will
72 decrease its pH less than for a sample with a lower TA value.

73 $$TA = [HCO_3^-] + 2\,[CO_3^{2-}] + [B(OH)_4^-] + [OH^-] + [HPO_4^{2-}] + 2\,[PO_4^{3-}] + \dots - [H^+] - [HSO_4^-] - \dots \quad (1)$$

74 From Eq. (1), we see the increased OH^- concentration in a treated seawater solution corresponds to a salt solution
75 with increased alkalinity relative to the starting salt solution. This increase in OH^- ion concentration rapidly
76 increases the seawater pH upon mixing, resulting in a shift of the dissolved inorganic carbon (DIC) speciation
77 towards carbonate (Eisaman et al., 2023):

78 $$OH^- + HCO_3^- \rightarrow H_2O + CO_3^{2-} \qquad\qquad (2a)$$
79 $$OH^- + CO_{2,aq} \rightarrow HCO_3^- \qquad\qquad (2b)$$

80 The concentration of dissolved CO_2 gas ($CO_{2,aq}$) in this alkalinity-enhanced seawater is less than it would be if it
81 were in equilibrium with atmospheric CO_2 (Equation 2b). Over the longer timescale required for air-sea gas
82 exchange - weeks to months (Wang et al., 2023) or months to years (He and Tyka, 2023) depending on location - the
83 disequilibrium in the surface ocean resulting from the alkalinity addition drives the invasion of atmospheric CO_2
84 into seawater (or lessens the outgassing of CO_2 from the surface ocean to the atmosphere), where it reacts with

carbonate and is stored primarily in the stable bicarbonate phase (Jones et al., 2014; Bach et al., 2023; Renforth and Henderson, 2017; Eisaman et al., 2023).

$$CO_{2,g} \rightarrow CO_{2,aq} \tag{3a}$$
$$CO_{2,aq} + CO_3^{2-} + H_2O \rightarrow 2HCO_3^- \tag{3b}$$

Under typical ocean conditions, after equilibrium has been reached, OAE results in an increase in the DIC in seawater on the order of 0.7-0.9 moles of DIC per mole of NaOH added, with a slightly increased pH relative to the initial value (He and Tyka, 2023).

It is possible that air-sea gas exchange will not completely drive the seawater pCO$_2$ to the initial unperturbed value before the seawater sinks into the ocean interior and loses contact with the atmosphere for hundreds to thousands of years. Therefore, the DIC anomaly relative to the alkalinity anomaly present when the seawater sinks into the ocean interior may be used to assess the effective impact of the OAE for capturing atmospheric CO$_2$ on the 0-100 year timescales that are most important for climate interventions.

In addition to the storage of atmospheric CO2 in the form of DIC, this process may have the potential to locally and transiently mitigate the elevated pCO2 associated with ocean acidification (NASEM, 2021; Cross et al., 2023; Butenschön et al., 2021). In a water body with a finite seawater exchange rate with the ocean, such as a semi-protected estuary or bay, alkalinity could be added in a controlled manner such that the combination of the rapid reactions described by Eq.(1) and the exchange/flushing rate with the open ocean result in the bay being held in steady-state at a target pH or aragonite saturation state value that is higher than its equilibrium value under conditions of ocean acidification. As this added alkalinity diffuses through the bay and makes its way to the open ocean, CO2 removal and storage as DIC would occur. By metering the rate of alkalinity addition to the bay to match the flushing rate, the pH or saturation state of the bay can be held at a constant target value. Even once equilibrium has been achieved in the open ocean, the pH and the carbonate ion concentration in the open ocean remains slightly higher than before the alkaline discharge. However, the absolute value of this pH increase after equilibrium has been reached is sufficiently small relative to the alkalinity and DIC increase that mitigating ocean acidification on a global scale with this method is unfeasible. For example, increasing the equilibrium pH value from 8.0 to 8.1 at a fixed pCO2 of 400 µatm (at 20 C and 35 salinity with no macronutrients) requires a TA increase of around ~620 µmol/kg-sw and a DIC increase of around 520 µmol/kg-sw. Using these numbers, mitigating OA over the entire 360 million km^2 surface of the ocean to a depth of 100 meters would require around 487 gigatons of cumulative CO$_2$ removal. Deploying SEA MATE in the ocean or coastal waters will require an understanding of carbonate chemistry in seawater in the ocean volume under consideration, as well as thresholds for safe operation. For example, at the point of alkaline dispersal where there is the maximum change in seawater chemistry, SEA MATE must control the rate of alkalinity addition relative to the rate of mixing and dilution in the ocean to avoid the precipitation of Mg(OH)$_2$ or CaCO$_3$ (Hartmann et al., 2023; Moras et al., 2022). While Mg(OH)$_2$ readily redissolves, an increase in turbidity due to precipitation may negatively affect marine organisms (Bainbridge et al., 2018; Broderson et al., 2017). By contrast, CaCO$_3$ will generally not redissolve in the surface ocean without biological mediation, and runaway precipitation, where alkalinity removed by precipitation exceeds that added by the OAE treatment, can occur under conditions of increased aragonite saturation state and increased nucleation sites in the water column (Moras et al., 2022). CaCO$_3$ precipitation could counteract the intended effect of the OAE intervention by removing alkalinity from the surface ocean and releasing CO$_2$ gas via Eq. 5 (Zeebe and Wolf-Gladrow, 2001):
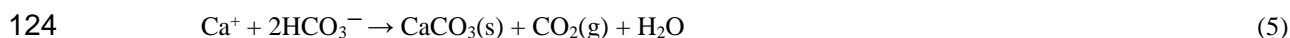
$$Ca^+ + 2HCO_3^- \rightarrow CaCO_3(s) + CO_2(g) + H_2O \tag{5}$$

Upon dispersal to the ocean through a coastal outfall pipe, the added alkalinity is advected and diffuses away from the point source, becoming increasingly diluted through the mixing zone. Because the timescale for air-sea gas exchange and re-equilibration described by Eq. (2) is longer than the characteristic timescale for dilution driven by

128 tides, currents, and weather, most of the CO_2 removal occurs far from the mixing zone. Dilution will spread the
129 impacts over a broad area, to an extent that it is unlikely that the impacts on the DIC distribution can be quantified
130 using only direct measurements, given current instrument resolution and the typical dynamic range of natural
131 variability (Wang et al., 2023). In general, options for measurement, reporting, and verification (MRV) of OAE will
132 therefore rely on (Ho et al., 2023): experimentation in laboratory and mesocosm settings, such as the work we
133 describe here, to establish CO_2 removal dynamics under conditions of OAE; direct monitoring of the rate and
134 characteristics of alkalinity addition into seawater; monitoring the seawater carbonate and environmental chemistry
135 in the immediate vicinity of the outfall via sensors and sampling (Cyronak et al., 2023; Schulz et al., 2023); and
136 ocean modeling to estimate CDR beyond the range of direct detection (Fennel et al., 2023).

137 While some work has investigated various aspects of NaOH-based ocean alkalinity enhancement in microcosms
138 (Ferderer et al., 2022; Hartmann et al., 2023), and mesocosms (Groen et al., 2023), and other work has studied the
139 release of NaOH over natural coral reefs as a method of local ocean acidification mitigation (Albright et al., 2016), a
140 systematic characterization of the efficiency and kinetics of OAE as a function of key process parameters has not yet
141 been performed. Here we report the first tank-scale tests of OAE that use aqueous hydroxide (NaOH) to enhance the
142 alkalinity of natural seawater, a process that mimics OAE via the electrochemical brine-to-alkalinity conversion
143 used in the SEA MATE process. Our experiments, conducted in 6,000 liter tanks using seawater pumped from Flax
144 Pond on Long Island Sound in Stony Brook NY, quantify the magnitude and timescale of the CO_2 removal from the
145 air and storage as seawater DIC by monitoring the air-seawater re-equilibration after an initial alkalinity
146 perturbation. In addition, our use of both laboratory-processed bottle samples and field-deployable sensors to
147 measure and over-constrain the carbonate chemistry response allows us to assess the suitability of certain sensing
148 platforms for MRV. Finally, we investigate safe thresholds for the rate and concentration of alkalinity addition to
149 avoid: (1) the precipitation and redissolution of $Mg(OH)_2$ that can lead to local, temporary increases in turbidity; and
150 (2) the precipitation of $CaCO_3$, which partially reverses the intended OAE effect by removing alkalinity from, and
151 releasing CO_2 gas into, the surrounding seawater.

152 Using this approach, we address the following key questions:

153 (1) How much additional atmospheric CO_2 is stored in seawater as DIC in response to a given alkalinity
154 perturbation?

155 (2) What is the timescale for CO_2 removal from the air, and how does it depend on pH and the magnitude of
156 alkalinity enhancement?

157 (3) What are the conditions for $Mg(OH)_2$ precipitation upon addition of NaOH to seawater?

158 (4) What are the threshold values for pH and aragonite saturation state beyond which undesired $CaCO_3$ precipitation
159 will occur?

160 Answering these questions is key to assessing the viability of this approach and to optimizing its eventual
161 deployment. The large tank experiments presented in this manuscript provide a stepping stone between bench-scale
162 experiments and in-situ mesocosms or field pilots. Even if these experiments simply confirm stoichiometric and
163 modeled expectations, this is critical information in the design and implementation of OAE deployments. This work
164 is a necessary part of the growing scientific body that will allow for field trials to progress.

165 **2. Methods**

166 **2.1 Experimental procedure**

167   We investigated the carbonate chemistry changes resulting from the addition of $NaOH_{(aq)}$ to natural seawater over
168   timescales ranging from 2 weeks to 2 months in a series of experiments at two scales: (1) two large (~6200 L)
169   indoor tanks, and (2) multiple 15 L aquaria (Fig. 1). The large volume of tank experiments allowed for precise
170   measurement of the seawater carbonate chemistry via bottle sampling (1L each, sent to NOAA/PMEL for analysis)
171   with high sampling frequency. To compliment these measurements, we also performed a series of experiments in
172   smaller aquaria (15 L each), which enabled a larger number of replicates and a faster time to equilibrium when
173   bubbled with air.

174
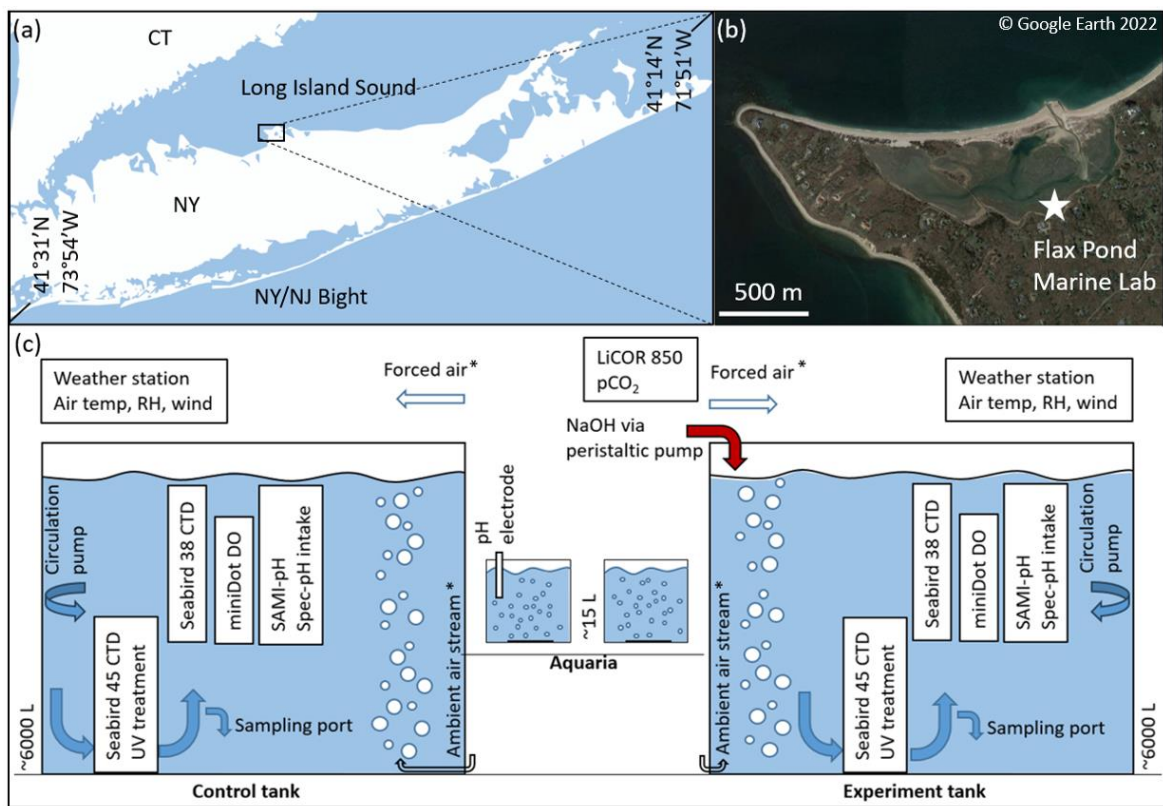
Figure 1: (*a, b*) Flax Pond Marine Laboratory is located on Long Island Sound, New York, USA (© Google Earth
2022). (*c*) The ~6000 L control and experiment tanks were instrumented with a series of oceanographic sensors and
sampled routinely for DIC/ TA analyses to allow for measurement of carbon uptake over time following an addition
of alkalinity in the form of NaOH. The ~15 L aquaria were instrumented with standard pH electrodes and monitored
with routine TA analyses. The Forced air* and Ambient air streams* indicate their use in some but not all
experiments, as noted in later sections.

181   This study was conducted at the Flax Pond Marine Laboratory at Stony Brook University, NY. All experiments used
182   natural seawater collected from Flax Pond, part of a 128-acre salt marsh tidal wetlands connected to the Long Island
183   Sound. The surface areas of the tanks and aquaria were ~4.6 m^2 and ~0.1 m^2, respectively. The tanks had a diameter
184   of 2.4 m, a total height of 1.52 m, and were typically filled to a height of ~1.35 m, allowing for a corresponding
185   seawater volume of 6185 L. The aquaria had a diameter of 0.3 m and were typically filled to a height of ~0.23 m, for
186   a total seawater volume of 15 L. The large tank volumes were chosen to limit interactions with walls while
187   increasing the air-seawater boundary, and to lose a smaller fraction of their volume to evaporation. These tanks
188   allow for in-situ oceanographic sensor deployment and frequent bottle sampling while retaining semi-controlled
189   temperature, mixing, filtration, and biological control. The inherent limitations of these tank tests include limited air-
190   sea interaction, unrealistic light levels and circulation, and biological responses that are not a perfect representation

191 of natural seawater in the ocean, but serve as a stepping stone to mesocosm and eventual field experiments. On
192 average, the large (~6,000 L) tank experiments took ~6.5 weeks after dosing with NaOH to reach 90% of the
193 calculated or extrapolated asymptotic ΔDIC/TA addition ratio indicative of full air-seawater equilibrium, as will be
194 discussed in Section 3. Therefore, in addition to the large tank tests, we conducted a series of smaller aquaria
195 alkalinity additions to increase our capacity for experimental test cases. The limitations of the aquaria include
196 limited sensor options, unrealistic circulation, and limited biological control. While it is expected that equilibration
197 occurs more rapidly in the small aquaria than in the large tanks, the results from these cases should be similar as
198 CO_2 equilibrates across the air-sea boundary. However, we note that some variation is expected due to limited
199 sensing and sampling options in the smaller aquaria and the greater potential for biological growth in the large tanks
200 over longer timescales.

201 **2.1.1 Tank experiments**

202 Seawater was pumped into the tanks at high tide through a series of sock filters to exclude macroscopic biology. The
203 tanks were then dosed to 40 ppm bleach (sodium hypochlorite) and the shock-treated seawater was allowed to
204 circulate through the tanks for ~1 day to limit biological growth. The seawater was then circulated through UV light
205 arrays to break down the bleach over ~1-2 weeks, as assessed by a standard Hach test kit for free chlorine. During
206 this period, seawater was pumped between the two large test tanks (~25 L/min) to increase mixing of the bleach and
207 to homogenize the tanks to similar initial conditions. For the remainder of each experiment, the seawater was
208 continually pumped through the UV sterilizers. Measurements of total alkalinity showed no significant differences
209 in the bulk seawater TA before and after the bleaching process in any experiment or control tank. In an early
210 experiment (in which bulk pH_T was raised from the initial condition to 8.7, as described below), the initial pH_T and
211 DIC varied between the control and experiment tanks by 0.17 and 77 μmol kg^{-1}, respectively. This was because
212 seawater was pumped from Flax Pond into multiple reservoirs and was then unevenly distributed between the tanks.
213 The experiments were subsequently refined to allow for several days of cross-pumping between tanks to
214 homogenize the control and experiment seawater before NaOH was added at the start of an experiment. More details
215 on experimental variations and a larger summary table are available in the Supplementary Materials.

216 Oceanographic sensors and discrete daily bottle sampling, as described in Sections 2.2 and 2.3, respectively, were
217 deployed for carbonate chemistry analysis for several days prior to the alkalinity addition to understand the initial
218 baseline conditions in both tanks. Two submerged pumps were used for water circulation within each tank: the first
219 pump (Current eFlux DC Flow Pump, 210 GPH) cycled seawater through the UV arrays with an estimated
220 overturning time of the bulk tank on order of 1 day, and a second (Kedsum Submersible pump, 260 GPH), mounted
221 at an angle halfway down the tank wall, allowed for subsurface circulation within the tank to reduce the occurrence
222 of unmixed 'dead zones ' and subsequent non-homogenous biological growth, as assessed visually on the surface of
223 the water and/or tank lining. Initial tank experiments were conducted with a still surface condition, i.e., with no
224 visible water movement across the surface of each tank. As experiments progressed, forced air movement was added
225 across the surface of each tank using a stationary fan with a wind speed of ~5 kph. This was done to control for
226 potential variations in the laboratory HVAC system and to potentially reduce the time to equilibration for the
227 experiments by increasing the rate of air-sea CO_2 equilibration. In later experiments, air was bubbled into the bottom
228 of each tank at a rate of ~ 30 L min^{-1} with an estimated surface area of ~ 0.3 m^2, with a goal of further increasing the
229 rate of equilibration to allow for more rapid throughput of experiments. These variations are further discussed in
230 Section 2.4.

231 After baselining, one tank (referred to as the "experimental tank") was dosed with enough 0.5 M NaOH (see
232 Supplementary Materials) to raise the bulk seawater pH to the target pH of interest for a given experiment, and the
233 same volume of DI water was added to the other tank (referred to as the "control tank"). NaOH additions were
234 typically dosed into the tank via peristaltic pump at a low enough rate (~50 mL/min) that a steady increase in bulk
235 tank pH was observed, but local pH measured just below the NaOH introduction never exceeded a pH of 9.0. A

236 pump (~25 L/min) was placed just below the NaOH stream to speed the mixing of NaOH into the bulk tank,
237 increase dilution from the point source, and to prevent the immediate precipitation of $Mg(OH)_2$ upon contact of the
238 NaOH with seawater. This pump was removed after the full volume of NaOH was mixed into the tank.

239 After the alkalinity addition, the tanks were left to equilibrate with the atmosphere and were monitored by sensors
240 and sampling as described in Sections 2.2 and 2.3. The tanks were indoors in the wet laboratory at Flax Pond Marine
241 Lab, such that temperature and CO_2 concentration were moderated by the building's HVAC system, but varied
242 throughout days and seasons depending on other uses of the lab space. The experiments were concluded when the
243 observed pH or DIC (calculated from daily pH and frequent TA measurements) appeared to stabilize (e.g., ΔpH
244 $\pm$0.05% or ΔDIC $\pm$10 μmol kg^{-1} per day) over several days. The continuous improvement of experimental methods
245 during this study resulted in some minor variations among the methods used for each experiment, including methods
246 of NaOH dosing, tank circulation, and biological control, as discussed where necessary in Section 3 and in the
247 Supplementary Materials.

248 **2.1.2 Aquaria experiments**

249 A series of polycarbonate aquaria were filled with 15 L of seawater taken from the large control tank just after the
250 described bleaching and bleach breakdown procedure was completed. NaOH was dosed into each aquarium to reach
251 a targeted bulk pH_T, with a corresponding volume of DI H_2O added to the control aquarium, and then the seawater
252 was allowed to equilibrate with atmospheric pCO_2 over days to weeks. The aquaria did not have either UV light
253 arrays for biological control or aquarium pumps for internal circulation. With the exception of a single target pH_T 8.5
254 experiment, all aquaria were bubbled with ambient air (~4 L min^{-1}) via a standard aquarium bubbling bar spanning
255 the center diameter of each aquarium, allowing for rapid CO_2 exchange . There was no fine control on air bubbling,
256 but the surface area of all air bubbles in a given aquarium at any point in time was estimated at ~0.01 m^2. No sensors
257 were deployed in the aquaria due to their limited size, and seawater chemistry was established via discrete pH_T and
258 TA measurements (Sect. 2.2). An optically clear lid was placed on each aquarium to reduce evaporation and
259 splashing onto nearby equipment. Some evaporation was evident from the rising TA throughout these experiments,
260 but was not resolvable within the resolution of a handheld salinometer used for these experiments. Temperature was
261 discretely recorded from a combination Ross pH electrode.

262 As shown in Eq. (6), we define the dimensionless 'Carbon-to-Alkalinity Ratio' (CAR) for our experiments as the
263 molar ratio of the increase in nDIC (in units of μmol/kg, normalized to the system's initial salinity to account for
264 evaporation) to the magnitude of the TA increase (ΔTA, in units of μmol/kg). nDIC$_{equ}$ is the measured (via direct
265 titration) or calculated (via CO2SYS using measured TA and pH_T) DIC value that the system reached at the end of
266 an experiment (Pierrot et al., 2006; Van Heuven et al., 2011). Some experiments were left long enough to achieve
267 equilibration with atmospheric CO_2, but others were halted early. In these cases, a CO2SYS calculation was used to
268 estimate the DIC increase expected at equilibration given initial seawater conditions, and the difference between this
269 value and the final recorded nDIC$_{equ}$ was used to estimate the overall percent equilibration for a given experiment.
270 Depending on experimental constraints described in later sections, nDIC$_i$ may represent either: (1) the final nDIC
271 measured (via titration of bottle samples) or calculated (via CO2SYS using seawater TA and pH) in the control tank,
272 or (2) the 'baseline' nDIC before the addition of NaOH to a given aquaria experiment, for cases where a
273 corresponding control case may not be available. Note that because we are reporting CAR values where the
274 measured DIC has reached or has been estimated at equilibrium, the CAR values we measure and report reflect the
275 ratio of ΔDIC to ΔTA that would be expected given sufficient time for air-sea exchange to reach equilibrium, and so
276 are equivalent to directly measuring the value of the "TA addition potential impact ratio" as defined by Wang et al.,
277 2023.

278 Carbon-to-Alkalinity Ratio (CAR) = (nDIC$_{equ}$ - nDIC$_i$) / ΔTA   (6)

2.2 Oceanographic sensors

Each tank was instrumented with a series of sensors placed halfway down the wall of the tank near the inlet of the UV circulation pump. A Seabird 38 Digital Oceanographic Thermometer and Seabird 45 MicroTSG Thermosalinograph continuously monitored seawater temperature and salinity, respectively. Dissolved oxygen was measured by a PME miniDOT Logger at 10 min resolution. pH_T was monitored daily by a SAMI-pH (manufacturer specified accuracy/precision ~ 0.003/0.001, though this accuracy is likely an underestimate of the uncertainty given known challenges for the calibration of the pH_T measurements) and by a semi-automated spectrophotometric (spec-pH) pH unit (~± 0.0055/0.0004) as described by Carter et al. (2013). CRM measurements were taken by each pH system at the beginning and end of each experiment and were used alongside discrete samples of DIC and TA as described in Section 2.3 to constrain the stability of each sensor. The SAMI-pH measurements were recorded at ambient seawater temperature and corrected for in-situ salinity as recorded by the Seabird Thermosalinograph following best practices from the manufacturer. The spec-pH analyses occurred in a jacketed cuvette held at 20 °C (regulated via water bath) and were corrected to the in-situ bulk tank temperature and salinity as recorded by the Seabird Thermometer and Thermosalinograph. Both the SAMI-pH and spec-pH rely on spectrophotometric analysis of metacresol purple indicator dye, which allows for pH measurement within the pH_T range of approximately 7 to 9. For experiments in which enough NaOH was dosed into seawater to raise pH above these limits, a Thermo Scientific Orion ROSS Ultra pH/ATC Triode combination electrode (8157BNUMD) was used to monitor pH_{NBS} at the surface of the tank (±0.01 precision), which was then converted to pH_T for comparison with the other pH sensor systems.

A LiCOR LI-850 sensor was used to analyze atmospheric pCO_2 (±1.5% accuracy) above the tanks. The inlet to this sensor was periodically moved between tanks to ensure that atmospheric pCO_2 in the vicinity of the control and experiment tanks was the same. AcuRite Iris weather stations were mounted on the side of each tank to monitor air temperature (±2 °C), relative humidity (±3%), and air speed (±0.8 m s^{-1}). All data were compiled on an hourly basis in a custom R package.

2.3 Discrete sampling

Two types of discrete sampling were used to constrain carbonate chemistry throughout these experiments. First, 500 mL of seawater was collected and preserved from each tank, typically on a daily basis, and as frequently as hourly during the addition of NaOH, following best practices laid out by Dickson (2007) including overflowing of the sample bottles during collection and addition of 0.2 mL of saturated mercuric chloride (HgCl$_2$) as a preservative. These bottle samples were analyzed for DIC and TA at NOAA Pacific Marine Environmental Laboratory (NOAA/PMEL). DIC concentrations were measured using a coulometer (UIC Inc.) and Single Operator Multiparameter Metabolic Analyzer (SOMMA) (Johnson et al., 1985). TA was determined by an open-cell acidimetric titration (Dickson et al. SOP 3b, 2007). The accuracy of DIC and TA measurements was assessed with Certified Reference Materials (CRMs, supplied by the Dickson laboratory at Scripps Institution of Oceanography), and overall uncertainty for both DIC and TA was typically ± 0.1% (~2 μmol/kg).

In addition, discrete seawater samples were analyzed for TA via open-cell potentiometric titration at Stony Brook University. A Thermo Scientific Orion ROSS Ultra pH/ATC Triode combination electrode (8157BNUMD), calibrated using three buffer solutions (pH_{NBS} 4.01, 7, and 10.01) was used to track the titration of a ~20 mL seawater sample with a dilute HCl solution (~0.1 M in 0.7 M NaCl, calibrated daily with CRM or a secondary seawater standard) following a modified Gran titration procedure using a Kloehn digital syringe pump (Song et al., 2020; Wang and Cai, 2004). The precision of TA measurements was ~±5-10 μmol/kg. This TA data was corrected to that of the bottle samples analyzed via titration at NOAA PMEL where available (see Supplementary Materials).

There are several differences between the aquaria experiments and the larger tank experiments. First, the aquaria experiments were monitored daily to every few days by discrete measurement of TA at Stony Brook University and

322 pHNBS via Thermo Scientific Orion ROSS Ultra pH/ATC Triode combination electrode (8157BNUMD) (±0.01
323 precision), which was then converted to pH$_T$ and corrected against the other pH sensor systems via occasional bottle
324 samples for DIC and TA analysis at NOAA PMEL. Variations between these experiments are noted in Section 3
325 where necessary and in the Supplementary Materials.

326 In either tank or aquaria cases where mineral precipitation was observed, 0.5 – 1 L of seawater was vacuum filtered
327 through a 0.45 μm Whatman GF/F filter via vacuum pump and the solids were rinsed with DI water 3 times to
328 remove NaCl. The precipitate was dried in an oven at 90 °C, then crushed into a uniform powder via mortar and
329 pestle. Samples were analyzed via Hitachi 4800 Scanning Electron Microscopy (SEM) (5 kV) and Rigaku SmartLab
330 X-ray Diffraction (XRD) (Cu Kα, 1.5406 Å, 10 - 100° 2 θ at 4°/min) at Brookhaven National Laboratory at the
331 Materials Synthesis and Characterization Facility of the Center for Functional Nanomaterials.

332 **2.4 Evaluation of CO$_2$ uptake by seawater in response to NaOH perturbation**

333 Seawater carbonate chemistry measurements were used to analyze the uptake of CO$_2$ in each tank, primarily relying
334 on calculations from the NOAA/PMEL DIC and TA analyses of bottle samples when available and using sensor pH
335 and Stony Brook TA measurements for cross-verification or to fill in between discrete DIC samples. DIC and TA
336 data were normalized to the salinity at the start of a given experiment to account for evaporation (Friis et al., 2003).
337 Carbonate chemistry calculations were then performed using CO2SYS (Lewis and Wallace, 1998), with Lueker et
338 al. (2000) carbonate constants, Dickson (1990) for KSO$_4$, and Lee et al. (2010) for total boron. Wherever possible, a
339 combination of CRM analyses and comparisons between simultaneous pH sensor and NOAA PMEL bottle samples
340 were used to correct SAMI-pH and spectrophotometric pH sensor data for drift.

341 Changes in the seawater carbonate chemistry over time were analyzed with respect to shifts away from the baseline
342 within a single control or experiment tank, as well as with respect to the differences between the control and
343 experimental tanks.

344 **3 Results and Discussion**

345 **3.1 Large tank experiments**

346 A summary of the range of oceanographic variables measured by sensors and bottle samples, calculated via
347 CO2SYS, or extrapolated to equilibration conditions during the large tank experiments is provided in Table 1. This
348 summary includes 6 experiments including 3 targeting pH$_T$ 8.5 (still surface water, with forced air, and with forced
349 air and air bubbling) and one (each) targeting pH$_T$ values of 8.7 (still surface water), 9.5 (with forced air and air
350 bubbling), and 10.3 (still surface water). While the initial seawater conditions were similar between the control and
351 experiment tanks, we note that these cases are not entirely comparable after the termination of cross-pumping
352 between tanks and the subsequent addition of alkalinity. While tanks were initially bleached, eventually some
353 biological growth was noted in each tank with potential differences in spatial and temporal distribution as well as
354 species and community differences. Herein, we assume that differences between the control and experiment cases
355 are due to the addition of alkalinity alone, but we note that characterization of other potential confounding factors is
356 a subject for future work.

357 The initial pH$_T$, TA, and DIC varied across experiments as seawater was collected between March 2022 and May
358 2023, ranging from pH 7.66 (December 2022) – 7.95 (May 2023), TA 2001 (May 2023) – 2176 (March 2023)
359 μmol/kg, and DIC 1847 (May 2023) – 2021 (March 2023) μmol/kg. Both measured and CO2SYS -calculated DIC
360 and TA values were normalized to salinity to account for evaporation, which drove salinity increases ranging from
361 0.2 – 7.1 across these experiments.

362 After the addition of NaOH, the control and experiment tanks were allowed to equilibrate with atmospheric CO_2.
363 While refinements in the experimental design allowed for complete or near-complete equilibration in later
364 experiments, as determined by the stabilization of nDIC at some asymptotic value, early experiments were
365 terminated before full equilibration. In all experiments, the absorption of atmospheric CO_2 began immediately after
366 the NaOH addition, as determined by decreasing pH and Ω_{arag} and increasing DIC and seawater pCO_2. nTA was
367 fairly stable or increasing (+10 - 60 µmol kg^{-1}) after the NaOH addition in all cases except the pH_T = 10.3
368 experiment, where nTA and DIC rapidly decreased due to runaway $CaCO_3$ precipitation. A stable TA value is an
369 indicator that no significant persistent mineral precipitation (e.g., $Mg(OH)_2$ or $CaCO_3$) has occurred. In the absence
370 of active mixing or bubbling, $Mg(OH)_2$ precipitation occurred immediately upon the introduction of NaOH to
371 seawater, however the precipitation can be rapidly dissolved by turbulence (i.e., pumping NaOH directly above a
372 strong circulation pump and/or stream of air bubbles). No $CaCO_3$ precipitation was observed in the tanks or aquaria
373 for which the bulk seawater pH_T was <10.0. The pH_T = 10.3 experiment was designed to induce $CaCO_3$ runaway
374 precipitation, as described in Section 3.3.

375 Ω_{arag} ranged from 1.4 - 2.5 in the control tanks with minimal variation over the course of any given experiment.
376 During the three experiments in which bulk pH_T was increased to ~8.5, Ω_{arag} increased immediately to 6.0 - 6.3 at the
377 peak of the experiments, before slowly decreasing to 2.8 - 3.0 as the seawater equilibrated with atmospheric CO_2.
378 For the bulk pH_T 9.5 experiment, Ω_{arag} increased to 20.2 and slowly decreased to 5.0 when the experiment was
379 ended at full equilibration. Mineral precipitation was observed in the bulk pH_T 10.3 experiment, where Ω_{arag} was
380 increased to 30.3 and rapidly (<1 week) fell to 5.2 after the addition of NaOH.

381 The results of one representative set of time-series measurements from the control and experiment tanks are shown
382 in Figure 2 for the case where pH_T of the bulk experiment tank was raised to 8.5 then allowed to relax into
383 equilibration with the atmosphere without the addition of surface air forcing or bubbling. Time-series plots for the
384 other tank-scale experiments are available in the Supplementary Materials.

385

386
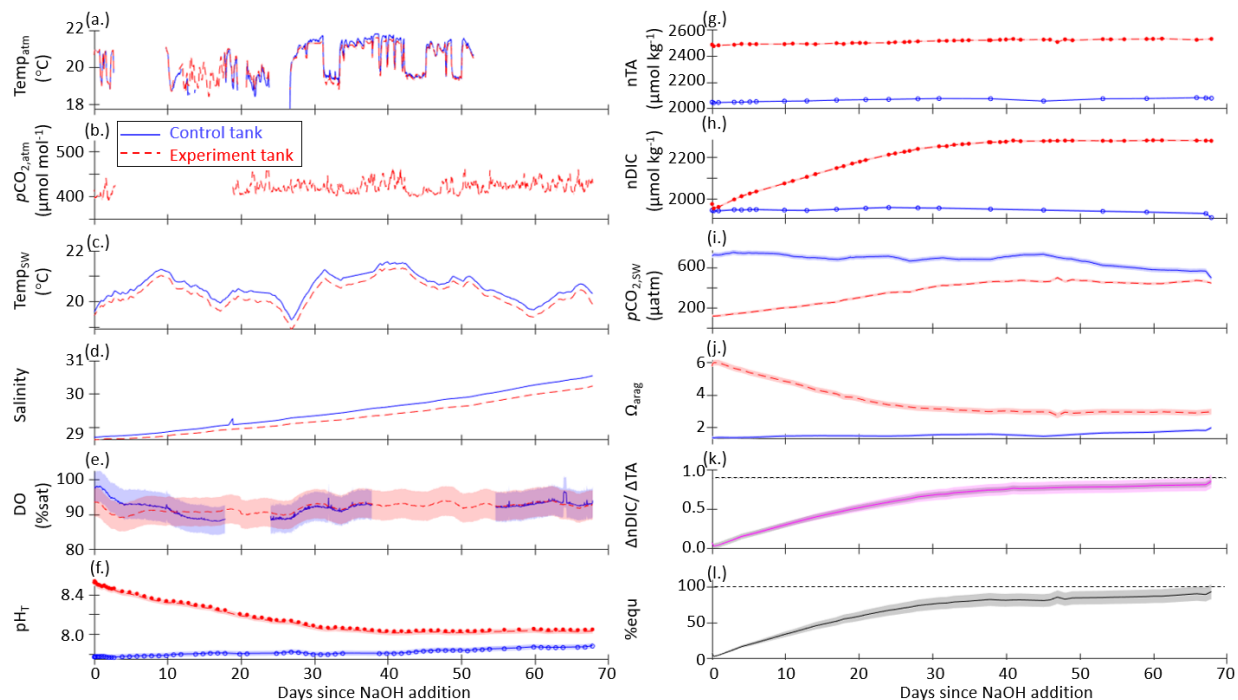
Figure 2: Time-series data for the case where pH_T of the bulk experiment tank was raised to 8.5 with no forced air flow and no bubbling (still surface) for control (blue, solid) and experiment (red, dashed) tanks: (*a*) continuously measured air temperature, (*b*) atmospheric pCO_2, (*c*) seawater temperature, (*d*) salinity, and (*e*) dissolved oxygen; (*f*) pH_T measured by the SAMI-pH (*circles*) and interpolated from the spec-pH (*line*), corrected to bottle sample and CRM data; (*g*) NOAA/PMEL-measured TA and (*h*) DIC from bottle samples and normalized to salinity; (*i*) seawater pCO_2 and (*j*) saturation state of aragonite (Ω_{arag}) calculated from interpolated nDIC and nTA data via CO2SYS; (*k*) the observed carbon uptake ratio (CAR) as ($nDIC_{exp} - nDIC_{control}$) / $\Delta TA_{NaOH\ addition}$ (*solid*) and the theoretical CAR (*dashed*) from a CO2SYS calculation using measured TA and the average $pCO2_{atm}$ to estimate the equilibrium change in DIC (*dashed*); (*l*) the percent equilibration estimated between the observed and theoretical CAR. Data gaps in panels *a*, *b*, and *e* are due to connectivity issues while offloading sensor data.

The ΔnTA and ΔnDIC values calculated between the control and experiment tanks are summarized in Figure 3where nTA and nDIC were interpolated between bottle samples measured at NOAA-PMEL, and/or were calculated via CO2SYS using sensor pH_T and TA measured at Stony Brook University corrected to less frequent NOAA-PMEL TA and DIC bottle samples. The ratio of the ΔnDIC to the addition of alkalinity in the form of NaOH, or ΔnTA, is included in Figure 3 for all experiments except that of the bulk pH_T increase to 10.3. Neglecting experiments that were terminated before full equilibration, the final observed CAR ranged from 0.75 ± 0.04 to 0.87 ± 0.08 (Table 1).

An anomalous event was noted in both the experiment and control cases for the target pH_T 8.5 experiment with forced air movement across the surface of the tank, wherein an increase in TA and DIC was noted around day 30 of the experiment. The cause of this event is unclear but could include biological changes in both tanks, the introduction of alkalinity from environmental contaminants, or the anomalous delayed release of alkalinity from suspended solids. This event was not observed in any other case, and highlights the importance of using controls to understand complex interactions in these experiments. A time-series including this event is available in the Supplementary Materials.

Henry's law and CO2SYS calculations were used to estimate the initial and final equilibration condition of each tank experiment. LiCOR $pCO_{2,atm}$ measurements were averaged across experiments to a representative value of 421 ± 14 ppm, which was used with the initial seawater temperature and salinity to estimate $pCO_{2,seawater}$ at the beginning of each experiment. This initial $pCO_{2,seawater}$ was in all cases greater than the atmospheric $pCO_{2,seawater}$, indicating that the seawater was not fully equilibrated with the atmosphere at the time when NaOH was added, likely due to respiration and decomposition of biology removed during the bleaching step (Section 2.1), and as such, the tanks should outgas CO_2. The initial equilibrium DIC was estimated from a CO2SYS calculation using the $pCO_{2,seawater}$ and nTA_i, which in all cases was less than the initial $nDIC$ measured or calculated from nTA_i and $pH_{T,i}$ (by $29 - 108$ μmol kg^{-1}). These observations underscore the importance of having a control tank to capture natural dynamics of CO_2 ingassing and outgassing to ensure that changes in DIC attributed to OAE are correctly accounted for.

The final equilibrium $nDIC$ was estimated from a CO2SYS calculation using the same $pCO_{2,seawater}$ and the nTA measured just after the NaOH addition, corrected for the linear increase in salinity over the course of the experiment. The ratio of the expected $\Delta nDIC$ calculated at equilibrium with the atmosphere to the addition of alkalinity provides a simple estimate of the expected CO_2 storage capacity for a given experiment. The percent equilibration for each experiment was then estimated from the measured and expected values for CAR. Within the series of experiments with a targeted pH_T of 8.5, the timeline to reach an estimated 90% CO_2 equilibration decreased from 65 days (with internal circulation but still water at the surface of the tank), to 50 days (with the addition of forced air movement across the surface of the tank) to 22 days (with the addition of air bubbling). We note that only the two cases (targeted pH_T of 8.5 and 9.5) with the addition of air bubbling reached full equilibration with the atmosphere.

Table 1: Range of variables measured, calculated, or extrapolated in large tank experiments, where M denotes direct measurement, C denotes calculation via CO2SYS, and E denotes extrapolation to equilibrium conditions. Subscripts *i* and *f* refer to initial and final conditions, and 'peak' refers to the time point immediately after the addition of NaOH.

pH target	-	8.5		8.5		8.5		8.7		9.5		10.3	
Surface condition	-	Still		Forced Air		Forced Air and Air Bubbles		Still		Forced Air and Air Bubbles		Still	
Tank (C = control, E = experiment)	-	C	E	C	E	C	E	C	E	C	E	C	E
ΔTA = NaOH addition (± 10 μmol/kg)	M	0	409	0	462	0	375	0	626	0	1406	0	3305
Salinity$_i$ (g/kg)	M	28.7	28.7	30.2	30.2	30.4	30.4	26.9	26.8	26.9	26.9	28.5	28.4
Salinity$_f$ (g/kg)	M	30.5	30.2	37.3	36.6	34.7	33.7	27.6	27.6	29.0	29.2	28.6	28.6
$pH_{T,i}$ (± 0.005)	M	7.76	7.76	7.73	7.73	7.93	7.93	7.92	7.75	7.95	7.95	7.70	7.75
$pH_{T,peak}$ (± 0.005)	M	-	8.54	-	8.58	-	8.49	-	8.68	-	9.51	-	10.10
$pH_{T,f}$ (± 0.005)	M	7.88	8.05	7.85	7.99	7.99	8.01	7.84	8.26	8.01	8.21	7.75	9.52
nTA_i (± 10 μmol/kg)	M	2049	2049	2069	2069	2248	2248	2075	2075	2007	2007	2023	2025
nTA_{peak} (± 10 μmol/kg)	M	-	2458	-	2531	-	2623	-	2701	-	3414	-	5330
nTA_f (± 10 μmol/kg)	M	2080	2528	2235	2674	2246	2624	2095	2696	2014	3363	2041	1253
$nDIC_i$ (μmol/kg)	M	1944	1947	1957	1996	2082	2087	1897	1975	1852	1852	1928	1938
$nDIC_f$ (μmol/kg)	M	1908	2280	2084	2433	2027	2365	1937	2336	1832	2977	1947	720
$\Omega_{aragonite,i}$	C	1.39	1.37	1.4	1.1	2.0	2.0	2.4	2.4	1.9	1.9	1.4	1.3
$\Omega_{aragonite,peak}$	C	-	5.9	-	6.0	-	6.2	-	8.8	-	19.3	-	30.3
$\Omega_{aragonite,f}$	C	2.0	3.0	1.7	2.8	2.5	3.0	1.9	4.4	2.1	4.9	1.4	5.2
CAR_f	C	-	0.85 ± 0.04	-	0.75 ± 0.04	-	0.87 ± 0.08	-	0.52 ± 0.07	-	0.82 ± 0.09	-	-
$CAR_{equilibrium}$	E	-	0.89	-	0.85	-	0.85	-	0.84	-	0.81	-	-
% equilibration (time elapsed in days)	E	-	95 ± 10 (67)	-	92 ± 10 (63)	-	102 ± 12 (45)	-	79 ± 6 (42)	-	104 ± 7 (74)	-	(13)

435
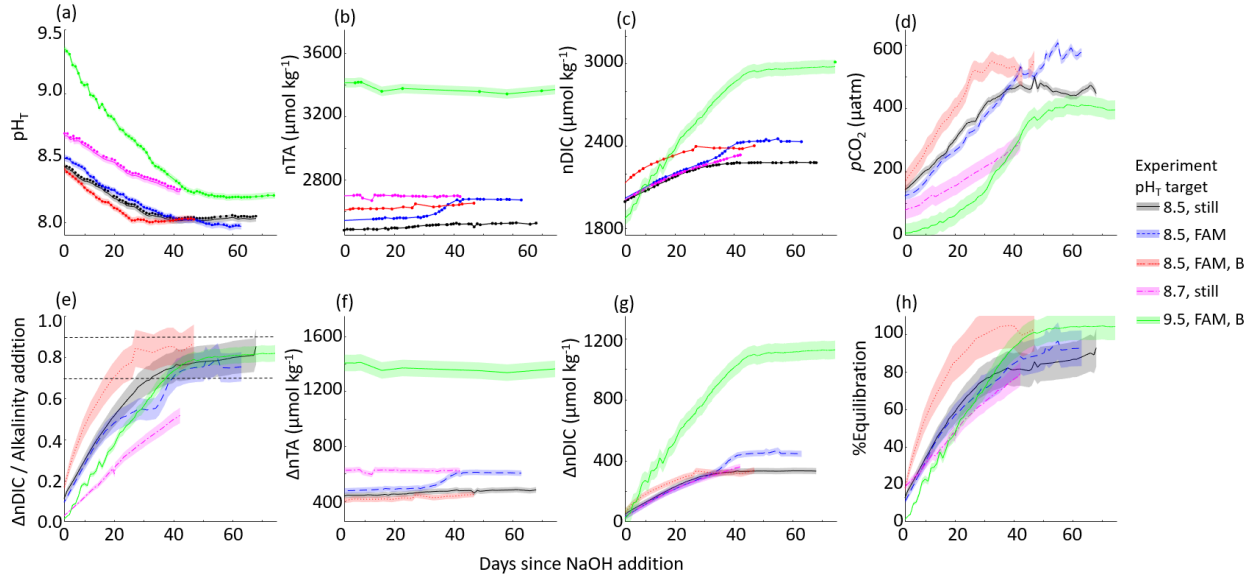
Figure 3: Results of 5 tank-scale experiments in which enough NaOH was added to each tank to raise the bulk pH_T to 8.3 – 9.7. pH_T decreased rapidly in all cases in which air bubbling sped equilibration with atmospheric CO_2. Results include: (a) measured pH_T, (b) measured nTA, (c) measured nDIC or CO2SYS calculated (for pH_T 9.5 case only), (d) CO2SYS -calculated pCO_2, (e) the observed carbon uptake ratio (CAR) as ($nDIC_{exp}$ - $nDIC_{control}$) / $\Delta nTA_{NaOH\ addition}$ with horizontal dashed lines representing the expected range of 0.7-0.9 mol CO_2 uptake / mol NaOH added to seawater, the change in (f) nTA and (g) nDIC compared to the baseline measurements before the addition of NaOH, and the percent equilibration estimated between the observed and theoretical CAR.

3.2 Aquaria experiments

Table 2 provides a summary of the range of oceanographic variables quantified for the aquaria experiments.

Table 2: Range of variables measured, calculated, or extrapolated in aquaria experiments, where M denotes direct measurement, C denotes calculation via CO2SYS, and E denotes estimation within specified equilibration conditions. Subscripts *i* and *f* refer to initial and final conditions, and 'peak' refers to the time point immediately after the addition of NaOH.

pH target	-	0 Control	8.3	8.5	8.5 Without air bubbles	8.7	9.3	9.5	9.7	9.9	10.0	10.1	10.2	10.3
ΔTA = NaOH addition ($\pm$ 10 µmol/kg)	M	0	187	331	362	543	1409	1679	2037	2216	2276	2504	2796	3829
$pH_{T,i}$ ($\pm$ 0.1)	M	7.94	7.97	7.90	7.86	7.95	7.98	7.98	7.98	8.06	8.04	8.04	8.04	7.95
$pH_{T,peak}$ ($\pm$ 0.1)	M	-	8.28	8.41	8.40	8.63	9.22	9.43	9.64	9.83	9.91	10.23	10.32	10.20
$pH_{T,f}$ ($\pm$ 0.1)	M	8.06	8.03	8.07	8.11	8.08	8.21	8.20	8.23	8.65	8.96	8.72	9.46	7.99
TA_i ($\pm$ 10 µmol/kg)	M	2265	2262	2250	2250	2250	2393	2393	2393	2531	2531	2531	2531	2250
TA_{peak} ($\pm$ 10 µmol/kg)	M	-	2449	2582	2611	2793	3801	4072	4430	4748	-	-	-	4608
TA_f ($\pm$ 10 µmol/kg)	M	2323	2476	2640	2645	2822	3837	4110	4420	4462	1702	1835	1537	2202
DIC_i (µmol/kg)	C	2089	2073	2091	2107	2070	2192	2192	2192	2282	2287	2287	2287	2067

DIC_f (µmol/kg)	C	2113	2246	2377	2382	2540	3372	3486	3877	3389	992	1244	671	2003
$\Omega_{aragonite,i}$	C	2.1	2.2	1.9	1.8	2.1	2.34	2.4	2.4	2.9	2.8	2.8	2.8	2.1
$\Omega_{aragonite,peak}$	C	-	4.2	5.5	5.5	8.1	19.5	23.1	27.0	29.8	30.2	30.9	32.4	38.9
$\Omega_{aragonite,f}$	C	2.4	2.7	3.1	3.1	3.4	5.9	7.9	7.1	13.7	6.5	5.7	7.0	2.2
CAR_f	C	-	0.92 ± 0.10	0.87 ± 0.06	0.76 ± 0.05	0.87 ± 0.04	0.84 ± 0.02	0.86 ± 0.02	0.84 ± 0.02	0.50	-	-	-	-
$CAR_{equilibrium}$	E	-	0.69	0.67	0.64	0.77	0.80	0.80	0.80	0.81	-	-	-	-
% equilibration (time elapsed in days)	E	(40)	130 (16)	126 (18)	116 (40)	111 (16)	104 (18)	106 (18)	104 (18)	62 (1)	(1)	(1)	(1)	(16)
$CaCO_3$ precipitation?	M	-	No	No	No	No	No	No	No	No	Yes	Yes	Yes	Yes

The aquaria experiments are not directly comparable to the control stated in Table 2. Seawater for one control aquarium was collected in March 2023, and was monitored for pH_T and TA changes through May 2023. Seawater for the experimental aquaria was collected in three batches between March, April, and May 2023, with only 4-6 aquaria experiments running in parallel within each set of experiments due to space and analytical throughput constraints. Because of this, the experiments started in March 2023 could be compared directly to the control (target pHT 8.3, 8.5, 8.5 still, and 8.7), but the rest of the experiments used different initial seawater than the control aquarium. The CAR for each aquaria experiment was therefore calculated from changes in DIC and TA between the initial 'baseline' condition and after the NaOH was added within a given aquarium, rather than between the experiment and control cases. The CAR ranged between 0.76 ± 0.05 and 0.92 ± 0.10, excluding cases where mineral precipitation was evident and for the pH_T 9.9 case where the experiment ended after one day due to a sensor logging failure. This wide range in ΔDIC/ ΔTA is likely due to the limited number of TA samples collected throughout these experiments (daily at best with no duplicates due to the limited volume), and the imprecision of electrode-based pH_T measurements relative to the SAMI-pH and spec-pH based measurements used in the large tank experiments.

No significant changes in salinity were recorded during these experiments as measured by a handheld salinometer with a range of 30 - 31. Therefore, DIC and TA were not normalized to salinity. Temperature values ranged from 19 - 21 °C during the experiments.

Similar to the large tank experiments, we used Henry's law and CO2SYS calculations to estimate the initial and final equilibration condition of each aquaria experiment. The same average $pCO_{2,atm}$ of 421 ± 14 ppm was used with the initial seawater temperature and salinity to estimate $pCO_{2,seawater}$ at the beginning of each experiment. The initial equilibrium DIC was estimated from a CO2SYS calculation using this $pCO_{2,seawater}$ and TA_i, which in all cases was less than the initial DIC calculated from TA_i and $pH_{T,i}$ (by 16 – 36 µmol kg^{-1}). This indicates that the seawater was not fully equilibrated with the atmosphere at the time when NaOH was added, likely due to respiration and decomposition of biology removed during the bleaching step (Section 2.1), and as such, the aquaria should outgas CO_2. The final equilibrium DIC was estimated from a CO2SYS calculation using the same $pCO_{2,seawater}$ and the TA measured just after the NaOH addition. The percent equilibration for each experiment was then estimated between the measured and predicted values for ΔDIC/ ΔTA. Due to the air bubbling, most experiments approached equilibrium with the atmosphere within 1-7 days, with the exception of the non-bubbled pH_T 8.5 experiment that took ~20 days. The surface water of this non-bubbled experiment was stagnant, and the water was only mixed via stirring just before taking pH and TA samples. Absorption of atmospheric CO_2 began immediately after the NaOH addition, as determined by decreasing pH_T. We note that there are significant uncertainties in these equilibrium estimates leading to estimates of >100% equilibration. These estimates would be better constrained with more continuous carbonate chemistry measurements, particularly seawater and atmosphere pCO_2 throughout the experiments that would allow for more direct calculation of air-sea CO_2 flux and equilibration, and finer control of bubbling and diffusion rates are necessary to define the timeline for equilibration within the aquaria.

483 Each aquarium was gently stirred during the addition of NaOH to prevent and/or redissolve $Mg(OH)_2$ precipitation.
484 No $CaCO_3$ precipitation was observed in the tanks below a bulk seawater pH_T of 10.0, and TA remained stable in
485 each of these experiments with the exception of some increase driven by minor evaporation on the order of +2
486 umol/kg per day. Experiments where $CaCO_3$ precipitation was induced by increasing the starting pH to values above
487 10 are discussed in Section 3.3.

488 The aquaria experiments with target pH_T from 8.3 – 9.9 are summarized in Figure 4.
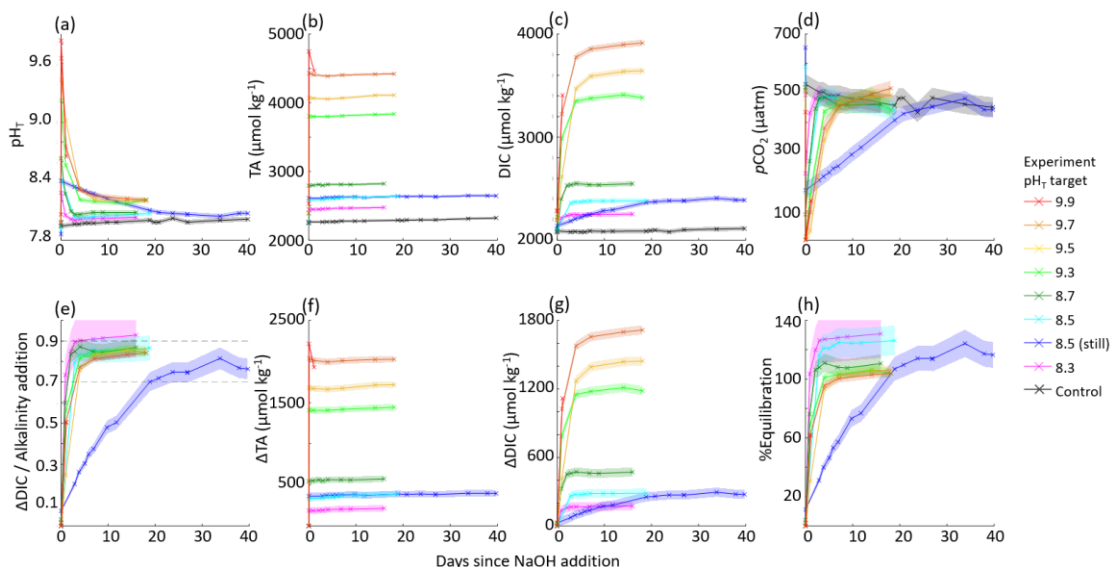
489

490 **Figure 4:** Results of 9 aquaria experiments in which enough NaOH was added to each aquaria to raise the bulk pH_T
491 to 8.3 – 9.9. pH_T decreased rapidly in all cases in which air bubbling sped equilibration with atmospheric CO_2.
492 Results include: (a) measured pH_T, (b) measured TA, (c) CO2SYS-calculated DIC, (d) CO2SYS-calculated pCO_2,
493 (e) the observed carbon uptake ratio (CAR) as $(DIC_{exp} - DIC_{baseline}) / \Delta TA_{NaOH\ addition}$ with horizontal dashed lines
494 representing the expected range of 0.7-0.9 mol CO_2 uptake / mol NaOH added to seawater, the change in (f) TA and
495 (g) DIC compared to the baseline measurements before the addition of NaOH, and the percent equilibration
496 estimated between the observed and theoretical CAR.

497 In general, the large tanks and aquaria showed reasonable agreement in achieving values for CAR within the
498 expected range of 0.7-0.9 (He and Tyka, 2023; Burt et al., 2021; Wang et al., 2023). While the use of aquaria
499 bubbled with air to speed equilibration allowed for a greater range of data collection within a constrained experiment
500 timeline, the quality of this data is limited by the lack of appropriate sensors to fit into these small 15 L aquaria and
501 fewer bottle samples due to the reduced quantity of seawater. However, while the large tanks allow for a larger
502 range of oceanographic sampling and sensing techniques, it is more challenging to fully quantify mixing and
503 circulation rates in the current large tank experimental setup.

504 Figure 5 shows the dependence of the equilibrium values of ΔDIC, CAR, and $\Delta pH_T = (pH_{final} - pH_{initial})$ as a function
505 of the alkalinity addition for both tank and aquaria experiments in which the final percent equilibration for CO_2 was
506 estimated at greater than 90%. Results for tank and aquaria experiments aligned well, with increasing ΔDIC for
507 increasing alkalinity additions. The CAR was observed for all experiments to fall within the range expected for
508 seawater with the temperature and salinity values used in these tests. As expected from calculations of the response
509 of the seawater carbonate buffer system to additions of alkalinity, the pH_T at equilibrium exceeded the initial pH_T
510 value prior to the addition of alkalinity. That is, even once equilibrium in the alkalinity enhanced experiment tank
511 had been reached, the ending pH value was slightly elevated relative to the starting pH value. This finding warrants

512 further investigation on the potential of OAE to mitigate some acidification impacts in controlled field trials by
513 metering the discharge of alkalinity to semi-protected water body.
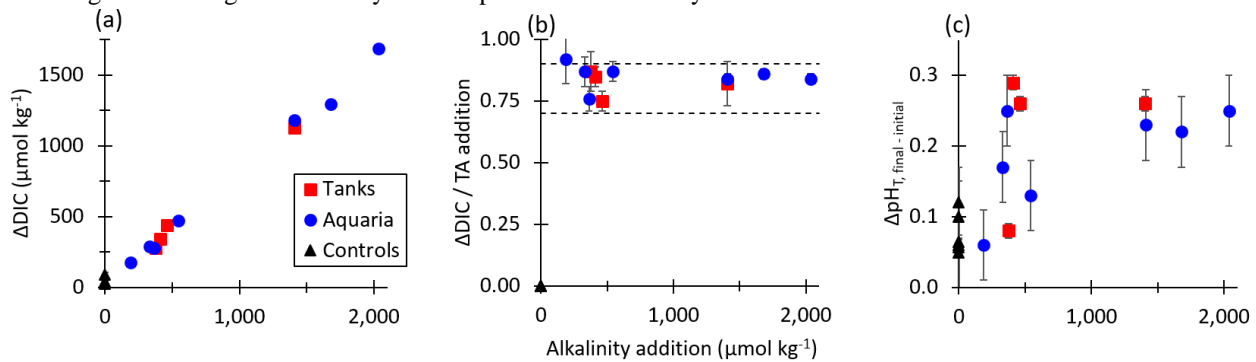
514
515 **Figure 5**: (a) The change in final CO2SYS-predicted DIC relative to the initial conditions for tank, aquaria, and
516 control experiments increases with increasing NaOH additions for cases where the air-sea CO_2 equilibration was
517 estimated at >90% at the termination of each experiment. (b) CO2SYS-predicted CAR (ΔDIC / Alkalinity addition)
518 at air-sea equilibrium conditions for tank, aquaria, and control experiments, with horizontal dashed lines
519 representing the expected range of 0.7-0.9 mol CO_2 uptake / mol NaOH added to seawater. (c) The measured ΔpH_T
520 = (pH_{final} – pH_{initial}) increases with

521 alkalinity addition for both tank and aquaria experiments.

3.3 Experiments exceeding the CaCO₃ precipitation threshold

523 While $Mg(OH)_2$ precipitation occurs immediately upon introduction of concentrated (i.e., ~0.5 M) NaOH to still
524 seawater, it may be rapidly dissolved or avoided entirely by gentle mixing, including via the use of stirrers,
525 circulation pumps, or air bubblers. This precipitation and redissolution happened rapidly enough that it was not
526 identified in any TA or other variables measured in the aquaria and tank tests. However, in cases where enough
527 NaOH was added to raise the bulk seawater pH_T to greater than 10.0 (i.e. in one large tank test with a target pH_T of
528 10.3, and in 4 aquaria experiments ranging from pH_T 10.0-10.3), runaway precipitation of $Mg(OH)_2$ and $CaCO_3$ was
529 observed. This was characterized by a sharp reduction in both TA and DIC and an increase in turbidity. Runaway
530 precipitation has been described as a condition in which more alkalinity is removed from seawater by mineral
531 precipitation than was initially added until a new steady state is achieved (Moras et al., 2022; Hartmann et al., 2023;
532 Suitner et al., 2023). This can significantly impact the efficiency of OAE, and has implications for biological
533 productivity, as increased turbidity may impact photosynthesis or predator-prey interactions.

534 In both the tank and aquarium pH_T 10.3 cases, discrete samples of the precipitate were collected at seven different
535 times after the bulk pH_T value reached 10.3 (0h, 3h, 24h, 49h, 71h, 145h, 167h - see Fig. 6) for XRD and SEM
536 analysis. At each timepoint, 0.5 – 1 L seawater was collected from the tank sampling port or from the center of the
537 aquaria. In cases where precipitation had visibly settled at the bottom of the aquaria, this material was stirred into the
538 water column before sampling. We note that material that settled to the bottom of the large tanks was not directly
539 collected, and that only a subset of precipitation was collected at each time point, such that later timepoints may
540 include solids that had precipitated at the beginning of the experiment. The filtered seawater was immediately
541 analyzed for TA and pH via Ross electrode because the heightened pH was out of the range of spectrophotometric
542 methods. Bottle samples of filtered seawater were not able to be analyzed at NOAA PMEL due to the continued
543 precipitation of $CaCO_3$ after filtration and preservation. Both XRD and SEM results showed the dominance of
544 $Mg(OH)_2$ precipitation immediately after the alkalinity addition and the corresponding increase in pH and $\Omega_{aragonite}$
545 (to a value of around 30). The $Mg(OH)_2$ precipitation at this stage was thick, slurry-like, and difficult to
546 appropriately rinse. Broad peaks associated with brucite in the 0 and 3 hr time points may reflect that these signals
547 were partially obscured by the presence of other salts, and a sharp peak in the 0 hr time point ~27° 2θ is likely

548 associated with NaCl. Within hours of the NaOH addition, the runaway $CaCO_3$ precipitation began, characterized by
549 fine, light particulates in the water column and a sharp increase in turbidity. Within ~24 hours of the NaOH addition,
550 most $Mg(OH)_2$ signals had disappeared, leaving only aragonite and calcite peaks in the XRD. The results of the
551 XRD analysis for the tank experiment are summarized in Figure 7, and the aquarium experiment showed similar
552 results (see Supplementary Materials). TA decreased throughout the precipitation of $Mg(OH)_2$ and $CaCO_3$, and was
553 below that of the initial seawater within 24 hours of the NaOH addition. In the tank experiment, the initial TA (2025
554 μmol/kg) was raised by 3305 μmol/kg. Within 3 days the TA had decreased to 1583 μmol/kg and continued to
555 decrease through the termination of the experiment to 1253 μmol/kg 10 days after the addition of NaOH. The DIC,
556 which was initially measured at 1938 μmol/kg, decreased to 720 μmol/kg by the end of the experiment. This
557 experiment shows that runaway $CaCO_3$ can result in a significant loss of both efficiency of alkalinity dosing for
558 OAE projects and of storage of carbon in the form of DIC. A figure of time-series data collected during the tank
559 experiment is available in the Supplementary Materials.
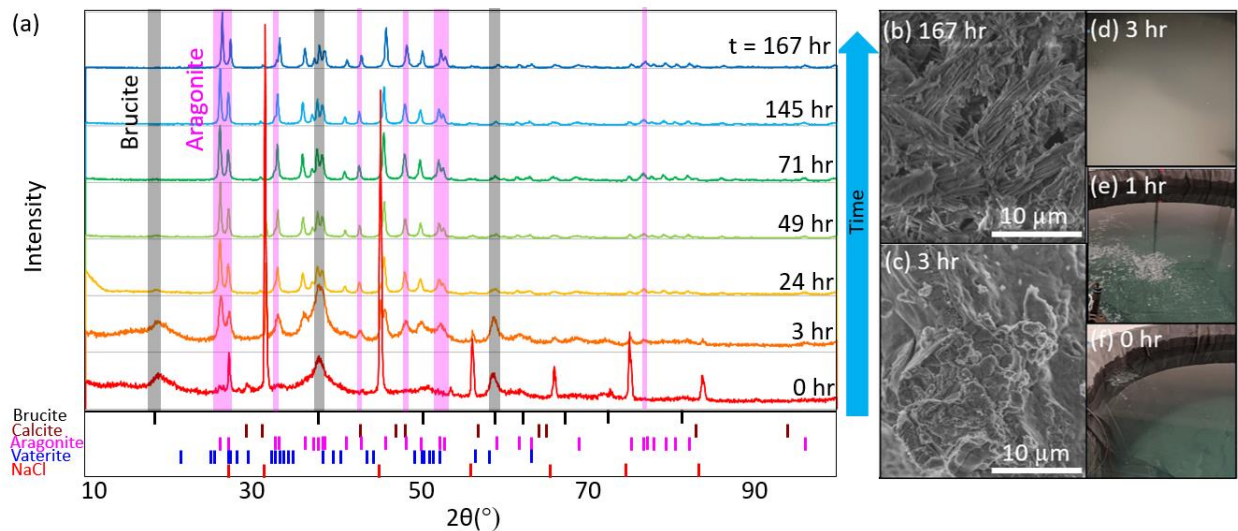
560

561 **Figure 6:** (*a*) XRD analysis of particulates filtered from seawater after the addition of enough NaOH to raise the
562 bulk seawater pH_T to 10.3 showed mineral precipitation initially dominated by $Mg(OH)_2$ before it was overtaken by
563 $CaCO_{3,arag}$. The shaded grey vertical bars highlight several peaks characteristic of brucite which typically disappear
564 after 24 hours, and the shaded blue bars represent several aragonite peaks which appear between 3 and 24 hours.
565 Representative SEM images show (*b*)$CaCO_{3,arag}$ at the end of the experiment, and (*c*) $Mg(OH)_2$ captured ~3 hours
566 after the NaOH addition. Photographs of the tank experiment show seawater (*d*) ~3 hours after the NaOH addition,
567 when runaway $CaCO_3$ precipitation became visually apparent, (*e*) during NaOH addition into still water (i.e.,
568 without the use of stirrers, circulation pumps, or air bubblers to break up and redissolve $Mg(OH)_2$), and (*f*) before
569 NaOH addition.

570 In summary, the presence and duration of brucite precipitation upon addition of 0.5 M aqueous NaOH depends on
571 the ratio of the NaOH addition rate to the local dilution rate in the receiving waters. Future research using flow
572 through tanks could help identify thresholds below which brucite precipitation can be avoided or limited, and the
573 immediate formation of $Mg(OH)_2$ may be reversible, as also noted by Suitner et al. (2023) and Cyronak et al.
574 (2023). At the given initial seawater conditions, the threshold for aragonite precipitation began at an Ω_{arag} of 30,
575 corresponding to $pH_T > 10.0$, and continued as Ω_{arag} decreased to ~5.2. This threshold corresponded to an increase in
576 TA of >2270 μmol/kg. The potential for runaway aragonite precipitation may be reduced by active mixing at the
577 point of NaOH introduction, maintaining a mixing volume below bulk seawater pH_T of 10.0, and allowing for
578 appropriate dilution in flow-through conditions, particularly on timescales of hours after alkalinity addition.

579 Additional characterization of runaway precipitation thresholds at varying temperatures, salinities, and suspended
580 particulate conditions will allow for OAE implementation designs that best avoid this potential risk to OAE
581 efficiency and ecosystem perturbation. We note that these results are only valid for experiments that are open to the
582 atmosphere allowing for exchange of CO_2 across the air-sea boundary using an aqueous hydroxide feedstock for
583 alkalinity, and are not comparable to experiments such as closed bottle incubations, where sustained conditions of
584 high Ω_{arag} may result in precipitation at different thresholds. We also note that we do not assume zero aragonite
585 precipitation at conditions below the stated thresholds, but that potential precipitation is not readily detectable with
586 our experimental setup. For example, heterogeneous $CaCO_3$ precipitation events, such as may occur on suspended
587 sediments in the water column, have been suggested through characteristic changes in seawater TA/DIC ratios in
588 cases of riverine inputs and bottom sediment resuspension (Bustos-Serrano et al., 2009; Wurgaft et al., 2016; 2021).
589 Suspended sediments in the context of OAE project sites could influence OAE efficiency and the potential for
590 runaway precipitation and should be included in future studies (Bach, 2023). The thresholds determined in this study
591 are significantly higher than those of some mineral-based OAE studies, including precipitation after an increase in
592 TA of ~500 μmol/kg using CaO and $Ca(OH)_2$ mineral additions (Moras et al., 2022). Hartmann et al. (2022) noted
593 precipitation resulting from alkalinity additions of >600 μmol/kg $Mg(OH)_2$, and found that alkaline solutions
594 avoided carbonate precipitation better than reactive alkaline particle additions to seawater. Suitner et al. (2023)
595 suggested that alkalinity additions > 2000 μmol/kg could be achievable given sufficient dilution to avoid runaway
596 precipitation. Together, these studies highlight the need to expand research into runaway precipitation to
597 characterize potential inefficiencies in OAE, particularly in in-situ experiments to establish relationships applicable
598 to ocean environments.

599 **5 Summary and Future Work**

600 These results demonstrate that ocean alkalinity enhancement using aqueous sodium hydroxide in seawater results in
601 CO_2 removal from air at an efficiency of 0.75 (± 0.04) – 0.92 (± 0.10), with 90% equilibration typically achieved
602 within 7 - 9 weeks (still surface water with ~16 L/min subsurface circulation through UV arrays) to 3 - 5 weeks
603 (with the addition of ambient air bubbling into the bottom of each tank) of the initial addition when performed in
604 ~6000 L tanks with seawater-air contact areas of around 4.6 m^2. These results are in general agreement with ratios
605 noted in Burt et al. (2021), He and Tyka (2023), and Wang et al., (2023). Here, uncertainties are driven by sensor
606 precision and temporal resolution in discrete DIC and TA sampling, the limited number of experiments with
607 minimal opportunities for duplicates or replicates, and poorly constrained data on mixing, circulation, and air
608 bubbling rates. Ongoing experiments seek to improve each of these conditions and should particularly focus on
609 constraining the movement of water within a given tank to improve air-sea equilibration estimates and to allow for
610 better extrapolation from tank to field experiments. In addition, a focus of ongoing and future work is to provide rate
611 estimates for the uptake of atmospheric CO_2 in response to an NaOH addition, allowing for fitting and extrapolation
612 of a shortened experiment to equilibration with the atmosphere.

613 We relied on several methods to constrain seawater carbonate chemistry. The tank-scale experiments primarily
614 relied on discrete (at most daily) DIC and TA sampling (NOAA PMEL), paired with daily measurements from
615 spectrophotometric pH systems (SAMI-pH and a semi-automated benchtop spec-pH system following Carter et al.
616 (2013)) and local TA measurements. With appropriate calibration or correction of the spec-pH systems relative to
617 CRM, there was no significant difference in carbonate calculations using the NOAA PMEL DIC-TA or spec-pH-
618 local TA pairings, though the latter case typically produced larger uncertainties. Aquaria experiments relied on a
619 standard glass pH electrode (at most daily, corrected to spectrophotometric systems) with discrete (at most daily) TA
620 measurements, which provided reasonable data relative to the tank experiments. As a result, ongoing tank-scale
621 experiments have limited the volume of discrete DIC and TA samples collected for analysis at NOAA PMEL to
622 allow for faster and less expensive monitoring via spec-pH and local TA titrations. However, we note that the major
623 limitation in this measurement pathway lies in the spec-pH method, which is typically limited to pH_T measurements
624 ranging from 7 – 9 for the meta-cresol purple indicator dye used. While our measurements retained some sensitivity

625 up to pH_T 9.5, such a method should typically be considered unreliable at these pH_T values, and we relied on

626 frequent correction to CRM and comparison with DIC/TA samples. Thymol blue is an alternative

627 spectrophotometric pH_T indicator dye with sensitivity over the higher pH_T conditions observed during these initial

628 trials and will be assessed for future experiments (Zhang and Byrne, 1996; Liu et al., 2006).

629 Aqueous NaOH with concentrations as high as 0.5 M can be added directly to turbulent seawater with only limited

630 observable precipitation of $Mg(OH)_2$. In these conditions this precipitated mineral rapidly redissolves on the

631 timescales of minutes to seconds. Improved control over the NaOH dosing rate (in our tank experiments, ~50 mL

632 NaOH/min) and the turbulence of the receiving water through metered flow through experiments will be valuable in

633 extrapolating to field conditions. This precipitation is detectable both visually and through turbidity measurements

634 and implies that straightforward measurement of pH and turbidity at the dispersal site can be used to adjust the

635 alkalinity dispersal rate according to local mixing conditions such that $Mg(OH)_2$ precipitation is avoided and/or

636 redissolves when it occurs. No significant $CaCO_3$ precipitation was observed at pH <10.0 or $\Omega_{aragonite} < 30.0$.

637 Runaway $CaCO_3$ precipitation was observed above these thresholds, where a massive precipitation and settling of

638 $Mg(OH)_2$ and $CaCO_3$ solids results in less alkalinity in the overlying water than at the starting condition. pH and

639 turbidity sensing combined with discrete TA measurements could be used as a feedback signal for alkalinity dosing

640 into seawater to ensure that the local maximum thresholds at the dispersal location do not approach or exceed

641 conditions that promote significant $CaCO_3$ precipitation. We note that future investigations seeking to better

642 approximate field conditions should take into account seasonal and tidal shifts in temperature and salinity, and

643 varying conditions of suspended sediment in the water column, including that of aerial dust, terrestrial runoff, and

644 resuspended bottom sediments.

645 In these experiments, the seawater was filtered and bleach treated prior to experiments to limit biological growth,

646 and both tank and aquaria experiments were conducted indoors with limited light. Nevertheless, in most

647 experiments, biological growth was observed after a few weeks, including cyanobacteria and coccolithophores. A

648 series of experiments are underway to test the difference in CO_2 removal efficiency for two side-by-side tanks, both

649 of which are dosed with NaOH, but only one of which was bleached. Preliminary results show minimal difference

650 between the bleached and unbleached tanks, indicating these experiments are applicable to real-world conditions, at

651 least for regions with biological communities similar to that of Long Island Sound, but further investigation is

652 warranted.

653 A focus of future work is to consider the potential impact of the SEAMATE process on local ocean acidification

654 mitigation efforts. We note that in each constrained tank and aquarium experiment, the pH_T at equilibrium exceeds

655 the initial pH_T value prior to the addition of alkalinity. A controlled release of alkalinity could theoretically be

656 configured to maintain a locally elevated pH_T value relative to pre-alkaline conditions, with potential uses in

657 aquaculture and hatchery environments.

658 These results provide clear and practical guidelines for MRV for OAE implementations employing aqueous

659 alkalinity. First, carbonate chemistry and turbidity measurements at the alkalinity dispersal location can ensure that

660 seawater parameters such as pH and $\Omega_{aragonite}$ remain within pre-determined safe bounds and that unwanted

661 precipitation is avoided. Second, for a given OAE deployment, where ocean models provide a reasonable certainty

662 about the fraction of the alkalinity plume remaining in the surface over weeks to months, the CO_2 removal efficiency

663 and timescale for air-seawater equilibration provided by our experiments can place a lower bound on the amount of

664 CO_2 removal expected from that OAE intervention. Expanding these studies from tank scale to mesocosm and field

665 experiments will be crucial to understanding biological impacts and constraining realistic air-sea interactions in

666 response to this type of OAE (Oschlies et al., 2023).

667 **Data availability**

668 Data are described in the manuscript and provided Supplementary Materials, which includes a .csv file with
669 processed sensor and sample time-series data at hourly resolution.

670 **Author contribution**

671 MDE and BRC designed the experiments and MCR carried them out with support from NH, CS, and XL. JH
672 provided support on experimental setup and instrumentation. MCR prepared the manuscript with contributions from
673 all co-authors.

674 **Competing interests**

675 MCR is Lead Oceanographer and Head of MRV at Ebb Carbon, Inc. MDE is Co-Founder and Chief Scientific
676 Advisor at Ebb Carbon, Inc.

677 **Acknowledgements**

678 We would like to than Stephen Abrams and Thomas Wilson at Stony Brook University Flax Pond Marine Lab for
679 technical assistance in experiment setup. We thank Chris Ikeda and Susan Curless of NOAA PMEL for support in
680 discrete sample analysis. We thank Mike Tyka for productive discussions. We thank Eyal Wurgaft for assistance in
681 TA titrations.

682 **Funding**

683 We acknowledge funding from The Grantham Foundation for the Protection of the Environment under the SEA
684 MATE (Safe Elevation of Alkalinity for the Mitigation of Acidification Through Electrochemistry) grant. In
685 addition, this research used the XRD facility of the Center for Functional Nanomaterials (CFN), which is a U.S.
686 Department of Energy Office of Science User Facility, at Brookhaven National Laboratory under Contract No. DE-
687 SC0012704. BRC and JH were funded through the Cooperative Institute for Climate, Ocean, and Ecosystem
688 Studies (CICOES) under NOAA Cooperative Agreement NA20OAR4320271 and supported by NOAA's PMEL.

689 **References**
690

691 Albright, R., Caldeira, L., Hosfelt, J., Kwiatkowski. L., Maclaren, J.K., Mason, B.M., Nebuchina, Y. et al.: Reversal
692   of ocean acidification enhances net coral reef calcification. Nature, 531, no. 7594: 362-365, 2016.
693 Bach, L.T.: The additionality problem of ocean alkalinity enhancement. Biogeosciences, 21, 261-277, 2024.
694 Bach, L. T., Gill, S.J., Rickaby, R.E.M., Gore, S., and Renforth, P.: CO_2 removal with enhanced weathering and
695   ocean alkalinity enhancement: potential risks and co-benefits for marine pelagic ecosystems. Frontiers in
696   Climate, 1, 7, 2019.
697 Bainbridge, Z.,Lewis, S., Bartley, R., Fabricius, K., Collier, C., Waterhouse, J., Garzon-Garcia, A., Robson, B.,
698   Burton, J., Wenger, A., and Brodie, J: Fine sediment and particulate organic matter: A review and case study on
699   ridge-to-reef transport, transformations, fates, and impacts on marine ecosystems. Marine Pollution Bulletin
700   135, pp. 1205-1220. 2018
701 Berner, R. A., Lasaga, A.C., and Garrels, R.M.: Carbonate-silicate geochemical cycle and its effect on atmospheric
702   carbon dioxide over the past 100 million years. Am. J. Sci.;(United States) 283, no. 7, 1983.
703 Boettcher, M., Chai, F. Cullen, J., Goeschl, T., Lampitt, R., Lenton, A., Oschlies, A. et al.: High level review of a
704   wide range of proposed marine geoengineering techniques. GESAMP Working Group Reports and Studies, 41,
705   2019.
706 Broderson, K.E., Hammer, K.J., Schrameyer, V., Floytrup, A., Rasheed, M.A., Ralph, P.J., Kühl, M., and Pederson,
707   O.: Sediment resuspension and deposition on seagrass leaves impedes internal plant aeration and promotes
708   phytotoxic Hh2S intrusion. Frontiers in Plant Science 8. 2017
709 Burt, D.J., Fröb, F., & Ilyina, T.: The sensitivity of the marine carbonate system to regional ocean alkalinity
710   enhancement. Frontiers in Climate 3, 624075. 2021

711   Bustos-Serrano, H., Morse, J.W., & Millero, F.J.: The formation of whitings on the Little Bahama Bank. Marine
712   Chemistry 113, no. 1-2, pp. 1-8. 2009
713   Butenschön, M., Lovato, T., Masina, S., Caserini, S., and Grosso, M.: Alkalinization scenarios in the Mediterranean
714   Sea for efficient removal of atmospheric CO2 and the mitigation of ocean acidification. Frontiers in Climate 3,
715   614537. 2021
716   Carter, B. R., J. A. Radich, H. L. Doyle, and A. G. Dickson.: An automated system for spectrophotometric seawater
717   pH measurements. Limnology and Oceanography: Methods, 11, no. 1: 16-27, 2013.
718   Caserini, S., Storni, N., & Grosso, M.: The availability of limestone and other raw materials for ocean alkalinity
719   enhancement. Global Biogeochemical Cycles, 36, e2021GB007246. https://doi. org/10.1029/2021GB007246,
720   2022.
721   Cross, J.N., Sweeney, C., Jewett, E.B., Feely, R.A., McElhany, P., Carter, B., Stein, T., Kitch, G.D., and Gledhill,
722   D..: Strategy for NOAA carbon dioxide removal research: A white paper documenting a potential NOAA CDR
723   science strategy as an element of NOAA's Climate Interventions Portfolio. NOAA Special Report. NOAA,
724   Washington, DC. DOI: 10.25923/gzke-8730. 2023Cyronak, T., Albright, R., and Bach, L.: Field experiments in
725   ocean alkalinity enhancement research. *State of the Planet*, 2-oae2023 (7). 2023.
726
727   de Lannoy, C.-F., Eisaman, M.D., Jose, A., Karnitz, S.D., DeVaul, R.W., Hannun, K., and Rivest, J.L.B.: Indirect
728   ocean capture of atmospheric CO_2: Part I. Prototype of a negative emissions technology. International journal of
729   greenhouse gas control, 70: 243-253, 2018.
730   Dickson, A. G.: An exact definition of total alkalinity and a procedure for the estimation of alkalinity and total
731   inorganic carbon from titration data. Deep Sea Research Part A. Oceanographic Research Papers, 28(6), 609–
732   623, 1981.
733   Dickson, A. G.: The development of the alkalinity concept in marine chemistry. Marine Chemistry, 40(1–2), 49–63,
734   1992.
735   Dickson, A.G.: Thermodynamics of the dissociation of boric acid in synthetic seawater from 273.15 to 318.15 K.
736   Deep Sea Research Part A. Oceanographic Research Papers, 37, no. 5: 755-766, 1990.
737   Dickson, A.G., Sabine, C.L., and Christian, J.R.: Guide to best practices for ocean CO_2 measurements. North Pacific
738   Marine Science Organization, 2007.Eisaman, M. D., Parajuly, K., Tuganov, A., Eldershaw, C., Chang, N.,
739   Littau, K. A. CO_2 Extraction from Seawater Using Bipolar Membrane Electrodialysis, Energy Environ. Sci., 5:
740   7346. https://doi.org/10.1039/c2ee03393c, 2012.
741   Eisaman, M. D.; Rivest, J. L. B.; Karnitz, S. D.; De Lannoy, C.-F.; Jose, A.; DeVaul, R. W.; Hannun, K. Indirect
742   Ocean Capture of Atmospheric CO_2: Part II. Understanding the Cost of Negative Emissions. International
743   Journal of Greenhouse Gas Control, 70: 254–261, https://doi.org/10.1016/j.ijggc.2018.02.020, 2018.
744   Eisaman, M. D., Geilert, S., Renforth, P., Bastianini, L., Campbell, J., Dale, A. W., Foteinis, S., Grasse, P., Hawrot,
745   O., Löscher, C. R., Rau, G. H., and Rønning, J.: Assessing the technical aspects of ocean-alkalinity-
746   enhancement approaches, in: Guide to Best Practices in Ocean Alkalinity Enhancement Research, edited by:
747   Oschlies, A., Stevenson, A., Bach, L. T., Fennel, K., Rickaby, R. E. M., Satterfield, T., Webb, R., and Gattuso,
748   J.-P., Copernicus Publications, State Planet, 2-oae2023, 3, https://doi.org/10.5194/sp-2-oae2023-3-2023, 2023.
749   Feely, R.A., Alin, S., Carter, B., Bednaršek, N., Hales, B., Chan, F., Hill, T.M., Gaylord, B., Sanford, E., Byrne,
750   R.H., Sabine, C.L., Greeley, D., Juranek, L., Chemical and biological impacts of ocean acidification along the
751   west coast of North America, Estuarine, Coastal and Shelf Science, doi: 10.1016/j.ecss.2016.08.043, 2016.
752   Feng, E. Y., Koeve, W., Keller, D.P., and Oschlies, A.: Model-Based Assessment of the CO_2 Sequestration Potential
753   of Coastal Ocean Alkalinization. Earth's Future, 5, no. 12: 1252-1266, 2017.
754   Fennel, K., Long, M.C., Algar, C., Carter, B., Keller, D., Laurent, A., Mattern, J.P., Musgrave, R., Oschlies, A.,
755   Ostiguy, J., Palter, J.B., and Whitt, D.B.: Modeling considerations for research on Ocean Alkalinity
756   Enhancement (OAE). *State of the Planet*, 2-oae2023 (9). 2023. Ferderer, A., Chase, Z., Kennedy, F., Schulz,
757   K.G., and Bach, L.T..: Assessing the influence of ocean alkalinity enhancement on a coastal phytoplankton
758   community. Biogeosciences 19, no. 23: 5375-5399, 2022.
759   Friis, K.; Körtzinger, A.; Wallace, D. W. R. The Salinity Normalization of Marine Inorganic Carbon Chemistry
760   Data. Geophys. Res. Lett., 30 (2). https://doi.org/10.1029/2002GL015898, 2003.
761   Groen, A., Kittu, L., Ortiz Cortes, J., Schulz, K., and Riebesell, U.: Assessing the response of particulate organic
762   matter stoichiometry to ocean alkalinisation. Ocean Visions Summit, Atlanta, Georgia, USA,
763   2023ocvi.conf27171G. 4-6 April 2023
764   Hartmann, J., Suitner, N., Lim, C., Schneider, J., Marín-Samper, L., Arístegui, J., Renforth, P., Taucher, J., and
765   Riebesell, U.: Stability of alkalinity in ocean alkalinity enhancement (OAE) approaches–consequences for
766   durability of CO_2 storage. Biogeosciences 20, no. 4: 781-802, 2023.

Harvey, L.: Mitigating the atmospheric CO_2 increase and ocean acidification by adding limestone powder to upwelling regions, Journal of 640 Geophysical Research: Oceans, 113, 2008.

He, J. and Tyka, M. D.: Limits and CO_2 equilibration of near-coast alkalinity enhancement, Biogeosciences, 20, 27–43, https://doi.org/10.5194/bg-20-27-2023, 2023.

Ho, D. T., Bopp, L., Palter, J.B., Long, M.C., Boyd, P.W., Neukermans, G., and Bach, L.T.: Monitoring, reporting, and verification for ocean alkalinity enhancement. *State of the Planet*, 2-oae2023 (12). 2023. Ilyina, T., Wolf-Gladrow, D., Munhoven, G., and Heinze, C.: Assessing the potential of calcium-based artificial ocean alkalinization to mitigate rising atmospheric CO_2 and ocean acidification, Geophysical Research Letters, 40, 5909-5914, 2013.

IPCC: Summary for Policymakers. In: Climate Change 2021: The Physical Science Basis, Contribution of Working Group I to the Sixth Assessment Report of the Intergovernmental Panel on Climate Change, edited by: Masson-Delmotte, V., Zhai, P., Pirani, A., Connors, S. L., Péan, C., Berger, S., Caud, N., Chen, Y., Goldfarb, L., Gomis, M. I., Huang, M., Leitzell, K., Lonnoy, E., Matthews, J. B. R., Maycock, T. K., Waterfield, T., Yelekçi, O., Yu, R., and Zhou, B.: Cambridge University Press, Cambridge, United Kingdom and New York, NY, USA, 3–32, https://doi.org/10.1017/9781009157896.001, 2022.

Isson, T. T., Planavsky, N. J., Coogan, L. A., Stewart, E. M., Ague, J. J., Bolton, E. W., et al.: Evolution of the global carbon cycle and climate regulation on earth. Global Biogeochemical Cycles, 34, e2018GB006061. https://doi.org/ 10.1029/2018GB006061, 2020.

Johnson, K.M., King, A.E., and Sieburth, J.M.: Coulometric TCO2 analyses for marine studies: An introduction. Marine Chemistry 16, pp. 61-82. 1985.

Jones, D.C., Ito, T., Takano, Y., and C.-W Hsu, C.-W.: Spatial and seasonal variability of the air-sea equilibration timescale of carbon dioxide. Global Biogeochemical Cycles, 28(11), 1163–1178, https://doi.org/10.1002/2014GB004813, 2014.

Kheshgi, H. S.: Sequestering atmospheric carbon dioxide by increasing ocean alkalinity, Energy, 20, 915-922, 1995.

Köhler, P., Hartmann, J., and Wolf-Gladrow, D.A.: Geoengineering potential of artificially enhanced silicate weathering of olivine. Proceedings of the National Academy of Sciences 107, no. 47: 20228-20233, 2010.

La Plante, E., Chen, X., Bustillos, S., Bouissonnie, A., Traynor, T., Jassby, D., Corsini, L., Simonetti, D., and Sant, G.: Electrolytic seawater mineralization and the mass balances that demonstrate carbon dioxide removal. ACS EST Engg. https://doi.org/10.1021/acsestengg.3c00004, 2023.

Lee, K., Kim, T.-W., Byrne, R.H., Millero, F.J., Feely, R.A., and Liu, Y.-M.: The universal ratio of boron to chlorinity for the North Pacific and North Atlantic oceans. Geochimica et Cosmochimica Acta 74, no. 6: 1801-1811, 2010.

Lewis, E., Wallace, D., & Allison, L. J.*:* Program developed for CO_2 system calculations. https://doi.org/10.2172/639712, 1998.

Liu, X., Wang, Z.A., Byrne, R.H., Kaltenbacher, E.A., and Bernstein, R.E.: Spectrophotometric measurements of pH in-situ: laboratory and field evaluations of instrumental performance. Environmental Science & Technology 40, no. 16, 5026-5044. 2006

Lu, X., Ringham, M., Hirtle, N., Hillis, K., Shaw, C., Herndon, J., Carter, B.R., and Eisaman, M.D.: Characterization of an Electrochemical Approach to Ocean Alkalinity Enhancement. In AGU Fall Meeting Abstracts, vol. 2022, pp. GC31C-01. 2022.

Lueker, T.J., Dickson, A.G., and Keeling, C.D.: Ocean pCO_2 calculated from dissolved inorganic carbon, alkalinity, and equations for K1 and K2: validation based on laboratory measurements of CO_2 in gas and seawater at equilibrium. Marine chemistry 70, no. 1-3: 105-119, 2000.

Minx, J.C., Lamb, W.F., Callaghan, M.W., Fuss, S., Hilaire, J., Creutzig, F., Amann, T., et al.: Negative emissions—Part 1: Research landscape and synthesis. Environmental Research Letters 13, no. 6: 063001, 2018.

Montserrat, F., Renforth, P., Hartmann, J., Leermakers, M., Knops, P., and Meysman, F.J.R.: Olivine dissolution in seawater: implications for CO_2 sequestration through enhanced weathering in coastal environments. *Environmental Science & Technology* 51, no. 7: 3960-3972, 2017.

Moras, C.A., Bach, L.T., Cyronak, T., Joannes-Boyau, R., and Schulz., K.G.: Ocean alkalinity enhancement–avoiding runaway $CaCO_3$ precipitation during quick and hydrated lime dissolution. Biogeosciences 19, no. 15: 3537-3557, 2022.

National Academies of Sciences, Engineering, and Medicine. A research strategy for ocean-based carbon dioxide removal and sequestration. 2021.

National Academies of Sciences, Engineering, and Medicine. Negative Emissions Technologies and Reliable Sequestration: A Research Agenda. 2018.

822 Nduagu, E."Production of Mg(OH)$_2$ from Mg-silicate rock for CO$_2$ mineral sequestration. Dissertation for Abo
823   Akademi University, 2012.Oschlies, A., Bach, L., Rickaby, R., Satterfield, T., Webb, R. M., and Gattuso, J.-P.:
824   Climate targets, carbon dioxide removal and the potential role of Ocean Alkalinity Enhancement. *State of the*
825   *Planet,* 2-oae2023 (1). 2023.
826 Pierrot, D., Lewis, E., and Wallace, D.W.R.: MS Excel program developed for CO$_2$ system calculations.
827   ORNL/CDIAC-105a. Carbon Dioxide Information Analysis Center, Oak Ridge National Laboratory, U.S.
828   Department of Energy, Oak Ridge, Tennessee, 2006.
829 Rau, G.H.: Electrochemical splitting of calcium carbonate to increase solution alkalinity: Implications for mitigation
830   of carbon dioxide and ocean acidity. Environmental science & technology 42, no. 23: 8935-8940, 2008.
831 Renforth, P., and Henderson, G.: Assessing ocean alkalinity for carbon sequestration. Reviews of Geophysics 55,
832   no. 3: 636-674, 2017.
833 Rigopoulos, I., Harrison, A.L., Delimitis, A., Ioannou, I., Efstathiou, A.M., Kyratsi, T., and Oelkers, E.H. : Carbon
834   sequestration via enhanced weathering of peridotites and basalts in seawater. Applied Geochemistry 91: 197-
835   207, 2018.
836 Rueda, O., Mogollón, J.M., Tukker, A., and Scherer, L.: Negative-emissions technology portfolios to meet the 1.5°
837   C target. Global Environmental Change 67: 102238, 2021.
838 Rogelj, J., Popp, A., Calvin, K. V., Luderer, G., Emmerling, J., Gernaat, D., Fujimori, S., Strefler, J., Hasegawa, T.,
839   Marangoni, G., Krey, V., Kriegler, E., Riahi, K., van Vuuren, D. P., Doelman, J., Drouet, L., Edmonds, J.,
840   Fricko, O., Harmsen, M., Havlík, P., Humpenöder, F., Stehfest, E., and Tavoni, M.: Scenarios towards limiting
841   global mean temperature increase below 1.5 °C, Nat. Clim. Change, 8, 325–332, https://doi.org/10.1038/s41558-
842   018-0091-3, 2018.
843 Schulz, K. G., Bach, L. T., and Dickson, A. G.: Seawater carbonate system considerations for ocean alkalinity
844   enhancement research: theory, measurements, and calculations. *State of the Planet*, 2-oae2023 (2). 2023..
845 Shaw, C., Ringham, M.C., Lu, X., Carter, B.R., Eisaman, M.D., and Tyka, M.: Understanding the Kinetics of
846   Electrochemically derived Magnesium Hydroxide for Ocean Alkalinity Enhancement. In AGU Fall Meeting
847   Abstracts, vol. 2022, pp. GC32I-0713. 2022.
848 Song, S., Wang, Z.A., Gonneea, M.E., Kroeger, K.D., Chu, S.N., Li, D., and Liang, H.: An important
849   biogeochemical link between organic and inorganic carbon cycling: Effects of organic alkalinity on carbonate
850   chemistry in coastal waters influenced by intertidal salt marshes. Geochimica et Cosmochimica Acta 275:123-
851   139, 2020.
852 Suitner, N., Faucher, G., Lim, C., Schneider, J., Moras, C.A., Riebesell, U., and Hartmann, J.: Ocean alkalinity
853   enhancement approaches and the predictability of runaway preciptiation processes- Results of an experimental
854   study to determine critical alkalinity ranges for safe and sustainable application scenarios. EGUsphere
855   [preprint], https://doi.org/10.5194/egusphere-20223-2611, 2023
856 Tyka, M.D., Arsdale, C.V., and Platt, J.C.: CO$_2$ capture by pumping surface acidity to the deep ocean. Energy &
857   Environmental Science 15, no. 2: 786-798, 2022.
858 Van Heuven, S., Pierrot, D., Rae, J., Lewis, E., & Wallace, D.: MATLAB program developed for CO$_2$ system
859   calculations. ORNL/CDIAC-105b, 530, 2011.
860 Vitillo, J. G., Eisaman, M.D., Aradóttir, E.S.P., Passarini, F., Wang, T., and Sheehan, S.W.: The role of carbon
861   capture, utilization and storage for economic pathways that limit global warming to below 1.5° C." Iscience:
862   104237, 2022.
863 Wang, H., Pilcher, D. J., Kearney, K. A., Cross, J. N., Shugart, O. M., Eisaman, M. D., & Carter, B. R.: Simulated
864 impact of ocean alkalinity enhancement on atmospheric CO2 removal in the Bering Sea. Earth's Future, 11(1),
865 e2022EF002816, 2023
866 Wang, Z. A. and Cai, W. J.: Carbon dioxide degassing and inorganic carbon export from a marsh-dominated estuary
867   (the Duplin River): A marsh CO$_2$ pump. Limnol. Oceanogr. 49, 341–354, 2004.
868 Wolf-Gladow, D. A., Zeebe, R. E., Klaas, C., Körtzinger, A., & Dickson, A. G.: Total alkalinity: The explicit
869   conservative expression and its application to biogeochemical processes. Marine Chemistry, 106(1–2), 287–
870   300, 2007.
871
872 Wurgaft, E., Steiner, Z., Luz, B., and Lazar, B.: Evidence for inorganic precipitation of CaCO3 on suspended solids
873   in the open water of the Red Sea, Marine Chemistry, 186, pp. 145–155, 2016.
874 Wurgaft, E., Wang, Z., Churchill, J., Dellapenna, T., Song, S., Du,J., Ringham, M., Rivlin, T., and Lazar, B.:
875   Particle triggered reactions as an important mechanism of alkalinity and inorganic carbon removal in river
876   plumes, Geophysical Research. Letters, 48, e2021GL093178, https://doi.org/10.1029/2021GL093178, 2021

877   Zeebe, R.E., and Wolf-Gladrow, D.: CO2 in seawater: equilibrium, kinetics, isotopes. Vol. 65, Gulf Professional
878   Publishing. 2001.
879   Zhang, H., and Byrne, R.H.: Spectrophotometric pH measurements of surface seawater at in-situ conditions:
880   absorbance and protonation behavior of thymol blue. Marine Chemistry 52, no. 1, pp. 17-25. 1996